

Multicalibration for Modeling Censored Survival Data with Universal Adaptability

Hanxuan Ye¹ and Hongzhe Li¹

¹University of Pennsylvania

Abstract

Traditional statistical and machine learning methods assume identical distribution for the training and test data sets. This assumption, however, is often violated in real applications, particularly in health care research, where the training data (source) may under represent specific subpopulations in the testing or target domain. Such disparities, coupled with censored observations, present significant challenges for investigators aiming to make predictions for those minority groups. This paper focuses on target-independent learning under covariate shift, where we study multicalibration for survival probability and restricted mean survival time, and propose a black-box post-processing boosting algorithm designed for censored survival data. Our algorithm, leveraging the pseudo observations, yields a multicalibrated predictor competitive with propensity scoring regarding predictions on the unlabeled target domain, not just overall but across diverse subpopulations. Our theoretical analysis for pseudo observations relies on functional delta method and p -variational norm. We further investigate the algorithm's sample complexity and convergence properties, as well as the multicalibration guarantee for post-processed predictors. Our theoretical insights reveal the link between multicalibration and universal adaptability, suggesting that our calibrated function performs comparably to, if not better than, the inverse propensity score weighting estimator. The performance of our proposed methods is corroborated through extensive numerical simulations and a real-world case study focusing on prediction of cardiovascular disease risk in two large prospective cohort studies. These empirical results confirm its potential as a powerful tool for predictive analysis with censored outcomes in diverse and shifting populations.

1 Introduction

Traditional statistical and machine learning methods assume identical distribution for the training and test data sets. This assumption, however, is often violated in real applications, particularly in health care research, where the training data (source) may under represent specific subpopulations in the testing or target domain. For instance, researchers may collect data from several hospitals, and they are interested in predicting the survival probability or restricted mean survival time for patients with unlabeled health

records in a new hospital based on their characteristics. At a high level, we view those hospitals with labeled data as source domains and the new hospitals with unlabeled data as target domains. Here the samples from the source domains may not represent the samples from the target domain. Consequently, predicting the outcome in target domain by simply applying models trained on the source domains results in poor performance with uncalibrated predictions.

Using data from source domains different from target domains presents challenges due to various possible distribution shifts. One such shift is that the supports of the observed variables in two domains (which we refer to as *heterogeneous domains*) are different. Another shift is that the shift of joint distributions of the source and target data, entailing the *concept shift* (differences in conditional distribution (Moreno-Torres et al., 2012)) and *covariate shift* (difference in marginal distribution (Bickel et al., 2009)). One approach to obtaining valid statistical inferences under covariate shift involves inverse propensity score weighting (IPSW) (Rubin, 1974; Weisberg et al., 2009). The propensity score between a source and target population relates the likelihood of observing data under the two populations. They are used to reweight the samples from an observational source to resemble a randomly sampled target population. Despite its success in an array of scientific settings (Frangakis, 2009; Cole and Stuart, 2010), propensity score models may be misspecified. In addition, in the settings where we aim to perform prediction on many downstream target populations, we need a separate estimation procedure for each target population.

Alternatively, one may want to learn a single estimator that automatically adapts to source-to-target shifts, thus enabling efficient inferences on downstream target populations and achieving target-independent learning. One difficulty is that the model can achieve high overall prediction accuracy, it may perform less accurately in minority populations (Buolamwini and Gebru, 2018). The systematic biases for subpopulations exhibited by the prediction system may arise inadvertently due to underrepresentation in the data used to train a machine learning model: data from a certain minority population is less available than from the majority populations. To mitigate the systematic biases broadly enough to handle such an imbalance in the training data, we investigate the new notion of fairness named multicalibration that was originally proposed in the seminal work of Hebert-Johnson et al. (2018) and later extended by Kim et al. (2019, 2022).

Notably, given black-box access to an initial predictor (hypothesis) and a relatively small “validation set” of labeled samples, Kim et al. (2019) proposed a boosting algorithm that was able to audit the initial predictor (hypothesis) to assess whether it satisfies the notion of subgroup fairness, namely multicalibration. If not, the algorithm iteratively updates the predictor until the multicalibration condition is fulfilled. The resulting multicalibrated predictor can exhibit provable improvement in group-wise fairness. Furthermore, Kim et al. (2022) made a connection between multicalibration and target-independent learning through the concept named “universal adaptability”, demonstrating that, under appropriate conditions, learning a multicalibrated predictor on source data will yield efficient estimation of statistics on unseen target distributions. One privilege of the multicalibration boosting algorithm is that it makes no assumption about how the initial predictor is trained, regardless of whether it is faithfully good or adversarially chosen. This feature is particularly advantageous in practical scenarios where model clients may want to improve resulting predictions across the populations, even when they are

not privy to the inner workings of the prediction system.

Deng et al. (2023) proposed s -Happy multicalibration as a generalization of multicalibration, unifying many fairness notions and target-independent learning approaches. Their framework yields many applications, including the notion of uncertainty quantification fairness, conformal prediction under covariate shift, and missing data analysis. To get a better understanding of the development of multicalibration, we refer the readers to the excellent notes by Roth (2022) and the references contained therein for a comprehensive introduction. For completeness, we also remark some related but different lines of work regarding calibration in survival analysis such as Goldstein et al. (2020); Kamran and Wiens (2021).

The multicalibration framework of Kim et al. (2019, 2022) is developed for binary classifications. In this paper, we develop a framework for multicalibration for modeling censored survival data. Survival analysis, which has been widely used in biomedical studies, explores the relationship between the characteristics of the individuals and their respective survival time. This relationship is often described by the survival or hazard function, which models the conditional distribution for event occurrence. The data in survival analysis are often (right) censored, rendering the ground truth of partial data unobservable, which poses a significant challenge in estimation and prediction tasks. New methods have been proposed to overcome these distribution shifts for survival data. Bellot and van der Schaar (2019) used boosting approach to select source samples that more resemble the target samples and discard dissimilar samples from the source domain. Li et al. (2023) accommodated time-varying heterogeneity in the risk estimation for both domains under the Cox model to improve estimation in the target, and Shaker and Lawrence (2023) extended survival domain adaptation to multiple source domains.

The goal of this paper is to develop a strong predictor for downstream analysis by only utilizing the labeled data in the source domains when the outcome is censored survival data. We mainly consider the scenario where source data differ significantly from target data due to a strong covariate shift. To deal with censoring, we apply the idea of pseudo observations (Andersen and Pohar Perme, 2010; Graw et al., 2009; Overgaard et al., 2017) based on the Jackknife method with consistent Kaplan-Meier estimators. Compared to other celebrated models like proportional hazards (Cox, 1972; Zhang et al., 2022) and accelerated failure time (Wei, 1992) models, pseudo observations facilitate the deployment of machine learning algorithms and allows for calibrating any initial estimator against these pseudo labels.

We develop an efficient algorithm specifically designed for modeling censored survival data, and thoroughly investigate its sample complexity and convergence properties by appealing to the functional delta methods and p -variational norm in analyzing the behavior of pseudo observations. We show how multicalibration implicitly anticipates propensity shifts to potential target distributions. This insight enables us to employ multicalibration as a tool for obtaining estimates in the target domain that achieve comparable or even better accuracy with estimator using propensity scoring.

2 Problem Setup

In survival analysis, we denote the time-to-event by T_i for individual i , and the censoring time by C_i . Therefore, the observed failure time is $\tilde{T}_i = T_i \wedge C_i$ given the right-censoring, and the censoring indicator is $\Delta_i = \mathbf{1}\{T_i \leq C_i\}$. Moreover, we let $X \in \mathcal{X} \subset \mathbb{R}^d$ be the d -dimensional covariates. Assume that we collect data in the source domain \mathcal{S} and target domain \mathcal{T} , and we use $D_i \in \{\mathcal{S}, \mathcal{T}\}$ as an indicator of domain membership. We denote observed data as $O_i = (X_i, \tilde{T}_i, \Delta_i, D_i)$ for each unit. With a little abuse of notation, we use $\mathcal{U}_{\mathcal{S}}$ and $\mathcal{U}_{\mathcal{T}}$ to denote the covariate distribution over unlabeled samples, conditional on D , i.e., $X|D = \mathcal{S} \sim \mathcal{U}_{\mathcal{S}}, X|D = \mathcal{T} \sim \mathcal{U}_{\mathcal{T}}$. Meanwhile, we use $\mathcal{D}_{\mathcal{S}}$ and $\mathcal{D}_{\mathcal{T}}$ to represent the joint distributions conditional on D , which are $(X, T, C)|D = \mathcal{S} \sim \mathcal{D}_{\mathcal{S}}$ and $(X, T, C)|D = \mathcal{T} \sim \mathcal{D}_{\mathcal{T}}$. Two estimands of interest, as considered by [Zeng et al. \(2021\)](#), are the at-the-risk function $\nu^{(1)}(T_i; t) = \mathbf{1}\{T_i \geq t\}$, and the truncation function $\nu^{(2)}(T_i; t) = T_i \wedge t$.

We have the following standard assumptions for censored survival data:

Assumption 1. *Given X_i , we have $(T_i, C_i) \perp\!\!\!\perp D_i | X_i$, i.e., the joint distribution of time-to-event and the censoring time is independent from the domain that an individual belongs to.*

Assumption 2. (a) *The joint distribution of time-to-event, covariates, and the domain an individual belongs to is independent from the censoring scheme: $\{T_i, X_i, D_i\} \perp\!\!\!\perp C_i$.*

(b) *A less stringent condition can be*

$$(T_i, X_i) \perp\!\!\!\perp C_i | \tilde{X}_i, \quad (1)$$

where \tilde{X}_i is some function of X_i , whose support comprising finite values.

Assumption 3. *The time-to-event is finite, bounded by some positive constant \tilde{C} : $T_i \leq \tilde{C}$.*

The above assumptions indicate that conditional on covariate X_i , i -th individual's survival time T_i does not depend on the domain (source or target) he/she belongs to. Meanwhile, the censoring should be independent, or at least conditionally independent from other variables (Assumption 2). Here, we adopt assumption $(T_i, X_i) \perp\!\!\!\perp C_i | \tilde{X}_i$ from [Overgaard et al. \(2019\)](#) instead of using strong assumption $T_i \perp\!\!\!\perp C_i \perp\!\!\!\perp D_i | X_i$, where \tilde{X}_i may be a subset of or coarser of X . For instance, \tilde{X}_i can be chosen as X_i when each component of X_i is binary. Subsequently, we will demonstrate the adaptability of our method to covariate-dependent censoring scenarios. Assumption 3 imposes non-defective condition ([Davison, 2003](#)), putting zero probability on infinite survival time that $\mathbb{P}(T_i = \infty) = 0$.

The goal of this paper to predict or estimate $\tau^{(k)}(t) = \mathbb{E}_{\mathcal{D}_{\mathcal{T}}}[\nu^{(k)}(T_i; t)]$ for a target population using the data collected in the source population. For $k = 1$, $\tau^{(1)}(t)$ lies in $[0, 1]$ and is known as the expected survival probability, and for $k = 2$, $\tau^{(2)}(t)$ represent the expected restricted mean. Denote by $m^{(k)}(X; t) = \mathbb{E}[\nu^{(k)}(T_i; t) | X]$, where $m^{(1)}(X; t)$ lies in $[0, 1]$ and $m^{(2)}(X; t) \in [0, \tilde{C}]$ as per Assumption 3. Under these Assumptions, the

probability $\mathbb{P}(T, C, X, D)$ can be factored as $\mathbb{P}(X)\mathbb{P}(D|X)\mathbb{P}(T, C|X)$. We can express $\mathbb{E}_{\mathcal{D}_T}[\nu^{(k)}(T_i; t)]$ in terms of $m^{(k)}(X; t)$ and the conditional probability X given D ,

$$\begin{aligned} \mathbb{E}_{\mathcal{D}_T}[\nu^{(k)}(T_i; t)] &= \mathbb{E}_{X \sim \mathcal{U}_T}[m^{(k)}(X; t)] = \int m^{(k)}(X; t) f(X|D = \mathcal{T}) \mu(dX) \\ &= \int m^{(k)}(X; t) \frac{\Pr(D = \mathcal{T}|X) f(X)}{\Pr(D = \mathcal{T})} \mu(dX) \\ &= \int m^{(k)}(X; t) \frac{\Pr(D = \mathcal{T}|X) f(X) \Pr(D = \mathcal{S}|X)}{\Pr(D = \mathcal{T}) \Pr(D = \mathcal{S}|X)} \mu(dX) \\ &= \int m^{(k)}(X; t) \frac{\Pr(D = \mathcal{T}|X) \Pr(D = \mathcal{S})}{\Pr(D = \mathcal{S}|X) \Pr(D = \mathcal{T})} \frac{f(X) \Pr(D = \mathcal{S}|X)}{\Pr(D = \mathcal{S})} \mu(dX). \end{aligned}$$

Given the definition of $\sigma(X) := \Pr(D = \mathcal{S}|X)$ as the conditional membership probability, the above equation can be written as

$$\mathbb{E}_{\mathcal{D}_S} \left[\nu^{(k)}(T_i; t) \frac{1 - \sigma(X)}{\sigma(X)} \frac{\Pr(D = \mathcal{S})}{\Pr(D = \mathcal{T})} \right].$$

If assuming equal prior probabilities $\Pr(D = \mathcal{S}) = \Pr(D = \mathcal{T})$, in reference to [Kim et al. \(2022\)](#), the above equation reduces to

$$\mathbb{E}_{\mathcal{D}_T} [\nu^{(k)}(T_i; t)] = \mathbb{E}_{\mathcal{D}_S} \left[\frac{1 - \sigma(X)}{\sigma(X)} \nu^{(k)}(T_i; t) \right] = \mathbb{E}_{\mathcal{U}_S} \left[\frac{1 - \sigma(X)}{\sigma(X)} m^{(k)}(X; t) \right], \quad (2)$$

which rewrites the quantity of interest using the expectation over the source distribution.

3 Methodology

3.1 Pseudo-observations of survival data

Survival analysis has posed the challenge of dealing with censored data whose underlying true survival time T_i is unobservable. To address this, a common approach employs pseudo observations ([Graw et al., 2009](#); [Andersen and Pohar Perme, 2010](#); [Jacobsen and Martinussen, 2016](#)) constructed in a Jackknife ([Miller, 1974](#)) manner,

$$\hat{\theta}_i^{(k)}(t) = N\hat{\theta}^{(k)}(t) - (N-1)\hat{\theta}_{-i}^{(k)}(t), \quad (3)$$

given N instances, where $\hat{\theta}^{(k)}(t)$ is a consistent estimator for $\tau^{(k)}(t)$, and $\hat{\theta}_{-i}^{(k)}(t)$ is derived by excluding the i -th individual. Typically, a good choice for $\hat{\theta}^{(k)}(t)$ is based on the Kaplan-Meier estimator,

$$\hat{S}(t) = \prod_{\tilde{T}_i \leq t} \left(1 - \frac{dN(\tilde{T}_i)}{Y(\tilde{T}_i)} \right),$$

where $Y(s) = \sum_{i=1}^N \mathbf{1}\{\tilde{T}_i \geq s\}$ is the at the risk process, and $N(s) = \sum_{i=1}^N \mathbf{1}\{\tilde{T}_i \leq s, \Delta_i = 1\}$ is the counting process for the event.

Remark 1. For the covariate-dependent censoring case, we consider the censoring-weighted

pseudo-observations (Overgaard et al., 2019; Binder et al., 2014),

$$\hat{\theta}_i^{(k)}(t) = \frac{\nu^{(k)}(\tilde{T}_i; t) \mathbf{1}\{C_i \geq \tilde{T}_i \wedge t\}}{\hat{G}(\tilde{T}_i \wedge t | \tilde{X}_i)}, \quad (4)$$

where \tilde{X}_i corresponds to the one in (1) and $\hat{G}(u | \tilde{X}_i)$ is some consistent estimator of the censoring survival function. The modified weighted estimator, as shown in Overgaard et al. (2019), produces unbiased and asymptotically normal parameter estimates.

To accommodate covariate-dependent censoring, additional conditions in line with Overgaard et al. (2019) is needed.

Assumption 4. Define $H_{\tilde{X}}(s) = \mathbb{P}(C \geq s, T \geq s | \tilde{X})$ as the conditional survival probability for T and C , we have

$$H_{\tilde{X}}(t) = \mathbb{P}(C \geq t | \tilde{X}) \mathbb{P}(T \geq t | \tilde{X}) > 0$$

almost surely, for any t under consideration. Moreover, the covariate-dependent censoring either follows the additive hazard model such that $\Lambda_c(s | \tilde{X}) = \int_0^s \tilde{X}^\top dB(u)$, or the proportional hazard model $\Lambda_c(s | \tilde{X}) = \int_0^s \exp(\tilde{X}^\top \alpha_0) d\Lambda_c^0(u)$, with some vector function of cumulative parameters $B(\cdot)$, coefficient vector α_0 , and the baseline hazard function $\Lambda_c^0(\cdot)$. In addition, the hazard $\Lambda_c(s | \tilde{X})$ is twice differentiable.

With Assumption 4, Overgaard et al. (2019) provides estimators for $\hat{G}(s | \tilde{X}) = \prod_0^s (1 - \hat{\Lambda}_c(du | \tilde{X}))$ in (4), where $\hat{\Lambda}_c$ is the estimate for the true censoring hazard, e.g., the Breslow estimator derived from Cox regression under the proportional hazard censoring assumption.

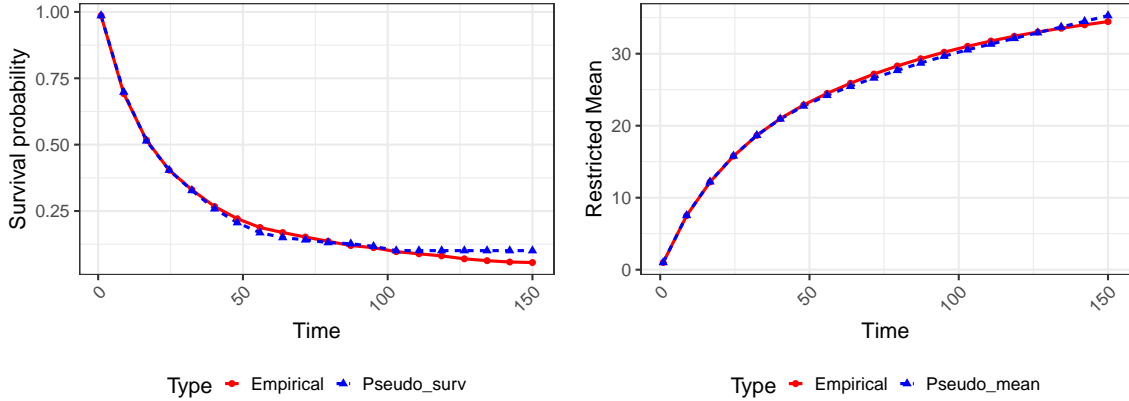


Figure 1: Illustrative examples of empirical curve derived under the assumption of known survival time, and the curve generated by averaging pseudo observations for 1000 sample points. The hazard follows Weibull distribution $\eta \nu t^{\nu-1} \exp(X_i^\top \alpha)$ where $\eta = 0.0001$, $\nu = 3$, $\alpha = (2, 1.5, -1, 1)^\top$, and the censoring times are uniformly distributed ($U([0, 115])$). The covariates (X_{i1}, X_{i2}) are jointly normal with mean zero, variance 2 and covariance 0.5, while X_{i3} and X_{i4} are binary with probability 0.4 and 0.5, respectively.

Straightforward estimators for expectations utilizing pseudo observations are expressed as

$$\widehat{m}^{(k)}(X; t) = \sum_{i=1}^N \widehat{\theta}_i^{(k)}(t) \delta_{X_i}, \text{ and } \widehat{\tau}^{(k)}(t) = N^{-1} \sum_{i=1}^N \widehat{\theta}_i^{(k)}(t),$$

for a specific time point t . Figure 1 gives an illustrative example demonstrating that the average $N^{-1} \sum_{i=1}^N \widehat{\theta}_i^{(k)}(t)$ evaluated at various time points can provide accurate estimates for the statistics of interest. Despite this, it is important to note that each individual pseudo observation per se may be noisy, fluctuating around the mean $m^{(k)}(X; t)$, as will be further discussed later.

3.2 Inverse propensity score weighting (ipsw)

When the source and target domain exhibit different marginal distributions $f(X)$, one must account for the covariate shift. In light of (2) and substituting $m^{(k)}(X; t)$ with its empirical counterpart $\widehat{\theta}_i^{(k)}(t)$ leads to the empirical inverse propensity score weighting (IPSW) estimator:

$$\widehat{\tau}^{(k)}(t) = \frac{\sum_{i=1}^N \widehat{\theta}_i^{(k)}(t) \frac{\sigma_{\mathcal{T}}(X_i)}{\sigma_{\mathcal{S}}(X_i)}}{\sum_{i=1}^N \frac{\sigma_{\mathcal{T}}(X_i)}{\sigma_{\mathcal{S}}(X_i)}},$$

where for clarity, we define $\sigma_{\mathcal{S}}(X) = \Pr(D = \mathcal{S}|X)$ and $\sigma_{\mathcal{T}}(X) = \Pr(D = \mathcal{T}|X)$.

Remark 2. *Our setup can be extended to more general cases. e.g., multiple source domains and a single target domain. Specifically, if we consider covariate distribution $f(X|D) = \sum_{m=1}^M f(X|D = \mathcal{S}_m) \mathbf{1}\{D = \mathcal{S}_m\}$ on source domain, then*

$$\widehat{\tau}^{(k)}(t) = \frac{\sum_{i=1}^N \widehat{\theta}_i^{(k)}(t) w_m \frac{\sigma_{\mathcal{T}}(X_i)}{\sigma_{D_i}(X_i)}}{\sum_{i=1}^N w_m \frac{\sigma_{\mathcal{T}}(X_i)}{\sigma_{D_i}(X_i)}},$$

where $w_m = \mathbb{P}(D = \mathcal{S}_m)$. Furthermore, it can be extended to the scenario with only one source domain and multiple target domains or to the one with multiple treatments.

In practice, however, the propensity scores are unknown, and many techniques varying in sophistication can be used to estimate the propensity score. The most common method used is via logistic regression. Formally, analysts seek an optimal fit $\widehat{\sigma}_{\mathcal{T}}$ from a fixed set of scoring functions Σ using unlabeled samples from source and target domains. Define $w(X) := \sigma_{\mathcal{T}}(X)/\sigma_{\mathcal{S}}(X)$, the reweighting of samples from $\mathcal{D}_{\mathcal{S}}$ is done according to the propensity odds $\widehat{w}(X) = \widehat{\sigma}_{\mathcal{T}}(X)/\widehat{\sigma}_{\mathcal{S}}(X)$,

$$\tau^{(k).ps}(t; \widehat{w}) = \mathbb{E}_{\mathcal{D}_{\mathcal{T}}} \left[\frac{\widehat{\sigma}_{\mathcal{T}}(X)}{\widehat{\sigma}_{\mathcal{S}}(X)} \nu^{(k)}(T_i; t) \right]. \quad (5)$$

However, it is crucial to acknowledge the potential misspecification in the estimated conditional membership probabilities, which might deviate from the true values. The discrepancy for some function $h(\cdot)$ relative to $w(X) = \sigma_{\mathcal{T}}(X)/\sigma_{\mathcal{S}}(X)$, for future use, can be measured via

$$d(h, w) = \mathbb{E}_{\mathcal{D}_{\mathcal{S}}} [|h(X) - w(X)|]. \quad (6)$$

e.g., $h(X) = \hat{w}(X) = \hat{\sigma}_{\mathcal{T}}(X)/\hat{\sigma}_{\mathcal{S}}(X)$. In survival analysis, (5) is not attainable since T_i s are not accessible for censored data, and more often, we use the empirical estimate

$$\hat{\tau}^{k,ps}(t; \hat{w}) = \frac{\sum_{i=1}^N \hat{\theta}_i^{(k)}(t) \hat{w}(X_i)}{\sum_{i=1}^N \hat{w}(X_i)}.$$

3.3 Multicalibration as an alternative to ipsw

An alternative strategy, also referred to as imputation, involves learning a function that correlates the responses (pseudo labels) with individuals' covariates only using the source data. The objective is to learn a function with good generalization capacity, which is competitive with the propensity score estimate, irrespective of the target population. As such, we can circumvent target-specific propensity scores using unlabeled samples from all domains. For concreteness, suppose $\tilde{m}^{(k)}(X; t)$ is some function learned for $m^{(k)}(X; t)$, and we define the prediction error for the target to be an absolute deviation from the true statistic

$$\text{Err}_{\mathcal{T}} = |\mathbb{E}_{\mathcal{U}_{\mathcal{T}}} \tilde{m}^{(k)}(X; t) - \tau^{(k)}(t)|, \quad (7)$$

which can be employed to measure the accuracy of predictors over the target domain. Additionally, within the context of algorithmic fairness (Dwork et al., 2012), the learned function should not only offer precise predictions but maintain fairness for subpopulations as well.

We introduce the concept of ‘‘Universal adaptability’’ to delineate the goal of learning a function comparable to IPSW. Following the definition of Kim et al. (2022), consider a set of conditional membership probability $\tilde{\sigma} \in \Sigma$, and define

$$\mathcal{H}(\Sigma) = \{\tilde{w} := \tilde{\sigma}_{\mathcal{T}}/\tilde{\sigma}_{\mathcal{S}}; \tilde{\sigma} \in \Sigma\}. \quad (8)$$

Definition 1 (Universal adaptability). *For a set of propensity scores Σ and a source domain distribution $\mathcal{D}_{\mathcal{S}}$, a predictor $\tilde{m}(X; t)$ is said to be (Σ, α) -universally adaptable if*

$$\text{Err}_{\mathcal{T}}(\tilde{m}^{(k)}(X; t)) \leq \text{Err}_{\mathcal{T}}(\tau^{(k),ps}(t; \hat{w})) + \alpha,$$

where $\hat{w} = \arg \min_{h \in \mathcal{H}(\Sigma)} d(h, w)$ is the best-fit approximation of w within the class $\mathcal{H}(\Sigma)$.

Universal adaptability characterizes a well-learned predictor \tilde{m} to be no worse than an IPSW estimator within a bias threshold α . This is a strong notion since accurate prediction on the source domain does not guarantee effective generalization on the target in general.

We next focus on the conditions and procedures to derive \tilde{m} that achieves universal adaptability. We introduce the notion of multicalibration (Hebert-Johnson et al., 2018; Kim et al., 2019; Roth, 2022), a property of prediction functions, initially studied in algorithmic fairness. By ensuring good calibration for the prediction function, we can guarantee overall accuracy and mitigate biases on structured populations of interest. We first define multicalibration for censored survival data parallel to regression and classification paradigms.

Definition 2 (Multicalibration). *For a given distribution \mathcal{D} and a class \mathcal{H} , a hypothesis (predictor) $\tilde{m}^{(k)}(\cdot; t) : \mathcal{X} \rightarrow [0, \tilde{C}]$ is (\mathcal{H}, α) -multicalibrated, if*

$$|\mathbb{E}_{\mathcal{D}} [h(X) (\tilde{m}^{(k)}(\cdot; t) - \nu^{(k)}(T_i; t))] | \leq \alpha, \quad \forall h(X) \in \mathcal{H}.$$

The definition of multicalibration involves a collection of real-valued functions \mathcal{H} , ensuring unbiased prediction across every (weighted) subpopulation defined by $h \in \mathcal{H}$. The merits of defining multicalibration in this way are two folds: First, it can be viewed as a generalization of the original definition in [Hebert-Johnson et al. \(2018\)](#) where the subpopulations of interest are defined in terms of a class of Boolean functions. For instance, h can take more forms like $h(X) = c(X)\mathbf{1}\{X \in G\}$ that combines some function $c(X)$ and subpopulation indicator $\mathbf{1}\{X \in G\}$, or $h(X) = h(X, m(X))$ that depends on function values, for more general purposes. Second, it allows for developing efficient black-box algorithms that agnostically identify function $h \in \mathcal{H}$ (auditing via regression), under which the current prediction violates multicalibration. As such, we do not have to examine all group combinations. Imaging \mathcal{G} being the collection of disjoint subpopulations of interest, it will be inefficient to take $2^{|\mathcal{G}|}$ inspections by permutating all the combinations.

A boosting style of the algorithm, `MCBoost`, is available online that can produce multicalibrated functions ([Pfisterer et al., 2021](#)) given a small portion of labeled data. However, the primary focus of the algorithm, implemented according to [Hebert-Johnson et al. \(2018\)](#); [Kim et al. \(2019\)](#), is for classification. Due to the censoring nature of true observations, we create time-varying pseudo observations via the Jackknife method, hoping they can play roles like true labels/responses. However, the pseudo observations bring about additional variations; their behaviors vary for event and censored data, and their boundedness is not guaranteed. Taking survival probability estimation as an instance, the pseudo observation can be either above 1 or below 0 for some individuals. For each individual, the pseudo observation curve may not be monotone as a function of t . Though clipping their values into $[0, 1]$ will ensure the boundedness, this yields a worse prediction. More insights on the curve of pseudo observation are referred to in Figure 3 of [Andersen and Pohar Perme \(2010\)](#). In contrast to classification, modeling our setting as a regression is more appropriate.

In this paper, we propose a modified multicalibration algorithm (Algorithm 1) tailored to censored data in survival analysis, based on gradient boosting ([Efron and Hastie, 2021](#)). Our algorithm employs a calibrating scheme against pseudo observations, whose range can be used to estimate unknown range \tilde{C} . In each step, we divide the observed variables into m buckets according to the values of the previously learned function $m^{(k),b}(\cdot; t)$, and apply an auditing function \mathcal{A} on each bucket to audit if it satisfies the notion of multicalibration. The buckets can also be fixed according to the values of the input $m^{(k),0}(\cdot; t)$ as well, which achieves multiaccuracy algorithm ([Kim et al., 2019](#)). To be more concrete, our algorithm iteratively searches a function $h \in \mathcal{H}$ using \mathcal{A} , on which the current predictor is mis calibrated, and then refine the predictor. The search for mis calibration is then reduced to a regression task over a class \mathcal{H} . The selection of regression algorithm for auditing \mathcal{A} is nuanced. The supplemental materials of [Kim et al. \(2022\)](#) exemplified linear functions $\{1 - \langle X, \omega \rangle : \omega \in \mathbb{R}^d\}$ as an effective approximation to the logistic propensity score odds $\exp(-\langle X, \omega \rangle)$ with performance similar to logistic regression propensity scoring, so that they employed ridge regression auditing to capture

Algorithm 1: Boosting for calibrating the censored data

Data: Initial estimator: $m^{(k),0}(X;t)$.
Accuracy parameter $\alpha > 0$; stepsize η .
Auditing algorithm \mathcal{A} .
Calibration set $D = \{(X_i, \tilde{T}_i, \Delta_i)\}, i = 1, \dots, N_1$.
Validation set $V = \{(X_i, \tilde{T}_i, \Delta_i)\}, i = N_1 + 1, \dots, N_1 + N_2$.

- 1 **for** $b = 0, \dots, B$ **do**
- 2 Compute buckets $\{S_k\}_{k=1, \dots, m}$, $S_k := \left\{x \in \mathcal{X} : m^{(k),b}(X;t) \in \left[\frac{(k-1)\tilde{C}}{m}, \frac{k\tilde{C}}{m}\right]\right\}$.
- 3 $h_{b,S_k}(X) \leftarrow \mathcal{A}\left(D, \left(m^{(k),b}(X_i;t) - \hat{\theta}_i^{(k)}(t)\right)_{S_k}\right)$.
- 4 $S^* \leftarrow \arg \max_{S_k} \frac{1}{|V|} \sum_{O_i \in V} h_{b,S_k}(X_i) \cdot \left(m^{(k),b}(X_i;t) - \hat{\theta}_i^{(k)}(t)\right)$.
- 5 $\Delta \leftarrow \frac{1}{|V|} \sum_{O_i \in V} h_{b,S^*}(X_i) \cdot \left(m^{(k),b}(X_i;t) - \hat{\theta}_i^{(k)}(t)\right)$.
- 6 **if** $|\Delta| > \alpha$ **then**
- 7 $m^{(k),b+1}(X;t) = m^{(k),b}(X;t) - \eta \cdot h_{b,S^*}(X)$.
- 8 **else**
- 9 **return** $\tilde{m}^{(k)}(X;t) = m^{(k),b}(X;t)$.

the shifts described by logistic propensity scores. In practice, we can use machine learning algorithms (ridge regression or decision trees) for auditing. More importantly, to prevent over fitting, we can fit a shallow tree or introduce a proper penalty. We also recommend using a smaller number of buckets m and step size η .

4 Theoretical Analysis

4.1 Property of multicalibration

We first introduce some notation. For two sequences of positive number $\{a_n\}$ and $\{b_n\}$, we write $a_n \lesssim b_n$ if $a_n \leq cb_n$ for some universal constant $c > 0$, and $a_n \gtrsim b_n$ if $a_n \geq c'b_n$ for some constant $c' > 0$. We say $a_n \asymp b_n$ if $a_n \lesssim b_n$ and $a_n \gtrsim b_n$. In addition, we use $a_n = O(b_n)$ to represent $a_n \leq Cb_n$, and $a_n = \Omega(b_n)$ to represent $a_n \geq C'b_n$, for some $C, C' > 0$. We say $a_n = \Theta(b_n)$ if $a_n = O(b_n)$ and $a_n = \Omega(b_n)$.

Our algorithm's guarantee for multicalibration under Definition 2 remains to be elucidated. Recall that the Definition 2 involves the auditing-related collection of functions \mathcal{H} , and indeed the richness of \mathcal{H} significantly impacts the calibration. We impose the following assumption that facilitates the theoretical analysis.

Assumption 5. *The auditing algorithm \mathcal{A} agnostically learns a symmetric class \mathcal{H} such that $|h(\cdot)| \leq C_{\mathcal{H}}$ for some positive constant $C_{\mathcal{H}} > 0$, for every $h \in \mathcal{H}$.*

Establishing the uniform bound involves bounding the empirical error from random samples and the error incurred from using the pseudo observations. By considering pseudo observations and their associated estimators as functionals, we can rigorously study them in the functional analysis framework (Dudley et al., 2011). The analysis of

pseudo observations is based on a von Mises expansion (Vaart, 1998; Graw et al., 2009; Overgaard et al., 2017). Specifically, we have the expansion

$$\widehat{\theta}_i^{(k)}(t) = \tau^{(k)}(t) + \dot{\phi}^{(k)}(\delta_{O_i} - F; t) + (N - 1)^{-1} \sum_{j \neq i} \ddot{\phi}^{(k)}(\delta_{O_i} - F, \delta_{O_j} - F; t) + R_{N,i}^{(k)}(t),$$

where $\tau^{(k)}(t)$, $k = 1, 2$ and O_i are defined as in Section 2, and the residual term $R_{N,i}^{(k)}$ is typically negligible. The first and second-order functional derivatives are denoted by $\dot{\phi}^{(k)}(\delta_{O_i} - F; t)$, $\ddot{\phi}^{(k)}(\delta_{O_i} - F, \delta_{O_j} - F; t)$, both of which are linear (bilinear) continuous operators. There is a correspondence between O_i and $\delta_{O_i} = (Y_i, N_{i,0}, N_{i,1})$, which comprises of three counting processes, where $Y_i(s) = \mathbf{1}\{\widetilde{T}_i \geq s\}$, $N_{i,0}(s) = \mathbf{1}\{\widetilde{T}_i \leq s, \Delta_i = 0\}$ and $N_{i,1}(s) = \mathbf{1}\{\widetilde{T}_i \leq s, \Delta_i = 1\}$. The limit distribution $F = (H, H_0, H_1)$ corresponds to the empirical distribution $F_N = N^{-1} \sum_{i=1}^N (Y_i, N_{i,0}, N_{i,1})$, with $H(s) = \Pr(\widetilde{T}_i \geq s)$, $H_0(s) = \Pr(\widetilde{T}_i \leq s, \Delta_i = 0)$, and $H_1(s) = \Pr(\widetilde{T}_i \leq s, \Delta_i = 1)$.

To study the pseudo observations rigorously in the functional framework, we apply a p -variation approach (Dudley and Norvaiša, 1999), wherein the p -variation norm we use is strong enough that the functionals of importance are sufficiently smooth but weak enough that the norm of empirical process converges sufficiently fast. The p -variation of a function $f : [a, b] \rightarrow \mathbb{R}$ is defined by $\|f\|_{[p]} = v_p(f; [a, b])^{1/p} + \|f\|_\infty$, where $\|\cdot\|_\infty$ is the supremum norm. The functional $v_p(f; [a, b]) = \sup \sum_{i=1}^m |f(x_{i-1}) - f(x_i)|^p$, where the supremum is over $m \in \mathbb{N}$ and points $x_0 < x_1 < \dots < x_m$ in interval $[a, b]$.

We restrict our analysis on $t \in \mathbf{T}$, a compacted domain within $[0, \widetilde{C}]$, and assume the uniform boundedness of the Lipschitz constant for functional derivatives:

Assumption 6. For $\forall t \in \mathbf{T}$, the linear continuous first-order functional derivative and the bilinear continuous second-order derivative have a uniform Lipschitz constant in the sense that $|\dot{\phi}^{(k)}(F; t)| \leq K_t \|F\|_{[p]}$ and $|\ddot{\phi}^{(k)}(F_1, F_2; t)| \leq K_t \|F_1\|_{[p]} \|F_2\|_{[p]}$ with $K_t \leq K$ for some universal constant K , where F, F_1, F_2 are some distribution functions.

The rationale behind this assumption is further discussed in the supplementary material. We do not consider t outside \mathbf{T} as $T \leq \widetilde{C}$ (Assumption 3), and the KM-estimator is significantly inaccurate for higher time values due to censoring.

The following theorem establishes a uniform bound on the deviation between the empirical estimate and the true value of the multicalibration statistics.

Theorem 3. Under Assumptions 1 and 3, consider Algorithm 1 that multicalibrates predictor against pseudo observations $\widehat{\theta}_i^{(k)}(t)$ s, which are derived according to (3) under Assumption 2(a), or according to (4) under Assumptions 2(b) and 4. Further, suppose \mathcal{A} agnostically learns a class \mathcal{H} satisfying Assumption 5, with ε -covering number $\mathcal{N}_\varepsilon = \mathcal{N}(\varepsilon, \mathcal{H}, \|\cdot\|_{L_1})$. Then given $\delta > 0$, fixed time point $t \in \mathbf{T}$, and N random samples, and any function $\check{m}^{(k)}(\cdot; t) \in [0, \widetilde{C}]$, it follows with probability at least $1 - \delta$ that:

$$\begin{aligned} & \sup_{h \in \mathcal{H}} \left| \mathbb{E}_{\mathcal{U}_S} [h(X)(\check{m}^{(k)}(X; t) - m^{(k)}(X; t))] - \frac{\sum_{i=1}^N h(X_i)(\check{m}^{(k)}(X_i; t) - \widehat{\theta}_i^{(k)}(t))}{N} \right| \\ & \leq 2\widetilde{C}C_{\mathcal{H}} \sqrt{\frac{\log(2\mathcal{N}_\varepsilon)/\delta}{N}} + \widetilde{C}\varepsilon + C_p \left(\frac{\log(1/\delta)}{N^{\frac{1}{p}}} + N^{\frac{1-p}{p}} \right) \end{aligned} \quad (9)$$

for some $p \in (1, 2)$.

The detailed proof is deferred to the supplementary material. The sample size N ought to be large enough so that the empirical average is close enough to the mean. From Theorem 3, we conclude

Corollary 4 (Sample Complexity). *Under the same conditions outlined in Theorem 3, to guarantee a uniform convergence over \mathcal{H} with error (9) at most $O(\alpha)$ with failure probability δ , the sample size is required to be $N = \Omega\left(\frac{\log(2\mathcal{N}_{\Theta(\alpha)/\delta})}{\alpha^2} + \left(\frac{1}{\alpha}\right)^{\frac{1}{\lambda}}\right)$, where $\lambda \in [1/4, 1/2)$.*

In the above Corollary, the $\lambda \in [1/4, 1/2)$ can be obtained if we choose $p \in [4/3, 2)$. It is noteworthy that we tend to obtain a higher sample complexity than standard classification and regression tasks due to the additional noise due to pseudo observations that potentially decelerates the convergence rate. The complexity of the function class \mathcal{H} plays an important role in determining sample complexity. Consider $\mathcal{H} = \{h_\theta(X), \theta \in \Theta \subset \mathbb{R}^d\}$, a class of functions satisfying Lipschitz condition and characterized by a compact parameter space Θ , which is often the case when we consider linear and logistic functions. In this scenario, the covering number $\mathcal{N}_\varepsilon \lesssim \left(1 + \frac{2\text{diam}(\Theta)}{\varepsilon}\right)^d$. Here, the complexity is dominated by $\alpha^{-\frac{1}{\lambda}}$, rendering it slower than the typical regression. On the other hand, if we consider $\mathcal{H} = \mathcal{C}([a, b]^d, B)$, a class of bounded convex functions defined over a compact domain, we have $\log \mathcal{N}_\varepsilon \lesssim \varepsilon^{-d/2}$, and $\frac{\log(2\mathcal{N}_{\Theta(\alpha)/\delta})}{\alpha^2}$ becomes the dominating factor (see the supplementary material for detailed discussion).

We further show that our Algorithm 1 must converge in finite iterations. The proof follows by showing that for an appropriately chosen step size η , every iteration improves the squared loss. Given the squared loss is lower bounded by 0 and upper bounded by the initial squared loss, the algorithm shall converge in a bounded number of updates. Formally,

Theorem 5 (Convergence Analysis). *Suppose \mathcal{A} agnostically learns a class \mathcal{H} satisfying Assumption 5. Let bias $\alpha > 0$ and $\delta > 0$, then with probability at least $1 - \delta$, Algorithm 1 converges to a (\mathcal{H}, α') -multicalibrate predictor $\tilde{m}^{(k)}(X; t)$ in $B = O\left(\frac{\ell_{\mathcal{D}_S(\tilde{m}^{k,0}(\cdot; t))}}{\alpha^2}\right)$ iterations at time point $t \in \mathbf{T}$, from $N = \Omega\left(\frac{\log(2\mathcal{N}_{\Theta(\alpha)/\delta}) + \log(B)}{\alpha^2} + \left(\frac{1}{\alpha}\right)^{\frac{1}{\lambda}}\right)$ samples, where $\alpha' = O(\alpha)$, and $\lambda \in [1/4, 1/2)$.*

4.2 Universal adaptability

The essence of multicalibration boosting lies in its ability to transfer weak learners to stronger learners by auditing the residuals, enabling enhancement in predictive accuracy across diverse subpopulations, which in turn improves the accuracy of statistical estimates within the target domain. How multicalibration leads to precise predictions under covariate shift needs to be elucidated in a formal mathematical language. Our main results relate the prediction error (7) obtained using multicalibration to that of IPSW. Specifically, we reveal that under proper conditions, a multicalibrated function $\tilde{m}^{(k)}(\cdot; t)$ leads to the property of universal adaptability. Recall the collection of propensity score odds \mathcal{H} defined in (8) and the specification error $d(h, w)$ defined in (6), with them in

place, we are ready to state the theorem below that establishes universal adaptability from multicalibration.

Theorem 6. *Under the same conditions outlined in Theorem 3, suppose $\tilde{m}^{(k)}(\cdot; t) : \mathcal{X} \rightarrow [0, \tilde{C}]$ is (\mathcal{H}, α') -multicalibrated over the source distribution \mathcal{D}_S , then for any target distribution \mathcal{D}_T , and any $\tilde{w} \in \Sigma$, $\tilde{m}^{(k)}(X; t)$ satisfies*

$$\text{Err}_T(\tilde{m}^{(k)}(X; t)) \leq \text{Err}_T(\tau^{(k).ps}(t; \tilde{w})) + \tilde{C} \inf_{h \in \mathcal{H}} (d(h, w) + d(h, \tilde{w})) + \alpha'.$$

If $\mathcal{H} = \mathcal{H}(\Sigma)$, $\tilde{m}^{(k)}(\cdot; t)$ is $(\Sigma, \tilde{C}d(\hat{w}, w) + \alpha')$ universal adaptable. Moreover, if $\tilde{m}^{(k)}(\cdot; t)$ is $(\mathcal{H}(\Sigma) \otimes \mathcal{C}, \alpha')$ -multicalibrated on the source domain, for some function class $\mathcal{C} \subset \{\mathcal{X} \rightarrow [0, \tilde{C}]\}$, $\tilde{m}^{(k)}(\cdot; t)$ is also $(\mathcal{C}, \tilde{C}^2 \inf_{\tilde{w} \in \mathcal{H}(\Sigma)} d(w, \tilde{w}) + \alpha')$ -multicalibrated on the target domain.

Theorem 6 also has implications beyond universal adaptability. It demonstrates that multicalibration in the source domain not only ensures universal adaptability but retains some degree of multicalibration over the target domain as well. Its statement can be simply understood as providing an adaptive guarantee under different degrees of shift: 1. If $\tilde{m}^{(k)}$ is well calibrated on the source domain, it will only lose a small amount in the multicalibration guarantee on targets close by. A simple instance is that $\mathcal{H}(\Sigma) = \{\text{Id}(x)\}$ in a scenario without any distribution shift. 2. Under extreme shifts, shifts that require the full power of the class to account for $\mathcal{H}(\Sigma)$, the universal adaptability and calibration guarantee weakens unless Σ is well specified and \mathcal{A} is capable of learning $\mathcal{H}(\Sigma)$ or $\mathcal{H}(\Sigma) \otimes \mathcal{C}$ agnostically. When Σ is accurately specified, i.e., $w \in \Sigma$, the discrepancy d diminishes, and the multicalibrated estimator is nearly unbiased.

Additionally, we can choose a more general class of $h(x) := h(x, m(x))$ that also depends on the function value. By enriching the class \mathcal{H} to incorporate odds functions $w \in \mathcal{H}(\Sigma)$ and approximations $p \in \mathcal{P} = \{p : \mathcal{X} \mapsto [0, \tilde{C}]\}$, we thus establish a connection between multicalibration with a L_2 prediction error $\mathbb{E}_{\mathcal{U}_T}[\tilde{m}^{(k)}(X; t) - m^{(k)}(X; t)]^2$, which is summarized in the following corollary.

Corollary 7. *Suppose $w(\cdot) \in \mathcal{H}(\Sigma)$ with $|w| \leq \tilde{C}$ and our algorithm reaches*

$$\sup_{\tilde{w} \in \mathcal{H}(\Sigma), p \in \mathcal{P}} |\mathbb{E}_{\mathcal{D}_S} \tilde{w}(X) (\tilde{m}^{(k)}(X; t) - p(X)) (\tilde{m}^{(k)}(X; t) - m^{(k)}(X; t))| < \alpha,$$

within $B = O(1/\alpha^2)$ iterations, where $p \in \mathcal{P}$ approximates the true $m^{(k)}(X; t)$, then

$$\mathbb{E}_{\mathcal{U}_T} [\tilde{m}^{(k)}(X; t) - m^{(k)}(X; t)]^2 \leq \alpha + \tilde{C}^2 \inf_{\tilde{w} \in \mathcal{H}(\Sigma), p \in \mathcal{P}} \{\|w - \tilde{w}\|_{L_2} + \|m^{(k)} - p\|_{L_2}\}.$$

In a nutshell, the multicalibrated prediction function, when evaluated on the unseen target domain, is nearly as good as the IPSW estimator, with only accessibility to the source samples. Therefore, by appealing to Algorithm 1, one can obtain a universally adaptable estimator. We defer further details and the technical proof of the theorem to the supplementary material.

5 Simulation valuations

We perform extensive simulations to evaluate the proposed methods and algorithms and to compare the results based on IPSW. Specifically, we consider the following models for generating the data:

- We model failure time according to the Weibull hazards model with hazard rate $\lambda(t|X_i) = \eta\nu t^{\nu-1} \exp(L_i)$, where $L_i = X_i^\top \alpha$. We also explore the scenario in which the failure time violates the proportional hazards assumption, specifying $\log(T_i) \sim \mathcal{N}(\mu, \sigma^2 = 0.64)$ with $\mu = 3.5 - X_i^\top \alpha$.
- Two censoring modalities are considered. The first is complete independent where $C_i \sim \text{Unif}(0, 120)$, and the second involves covariate dependence, with C_i following a Weibull model $\lambda^c(t|X_i) = \eta_c \nu_c t^{\nu_c-1} \exp(X_i^\top \alpha_c)$.
- We generate 5-dimensional covariates $X_i = (1, X_{i1}, X_{i2}, X_{i3}, X_{i4})^\top$, where $(X_{i1}, X_{i2})^\top$ are drawn from a mean zero bivariate normal distribution with correlation 1/4 and variance 2, $X_{i3} \sim \text{Binomial}(0.4)$, and $X_{i4} \sim \text{Binomial}(0.1X_{i3} + 0.2)$. The unbalanced categorical variables, mimicking practical variables like gender and race, anticipate a 40% female population, with minority proportions of 20% among females and 30% among males.
- To simulate adaptation from source to target domain, we initially consider a single source and target domain, setting the true membership probability odd as

$$\log(\sigma_S(X_i)/\sigma_T(X_i)) = X_i^\top \omega,$$

where $\omega = (0, 0.5, 0.45, -0.9, -0.7)^\top$. For scenario with two source domains, this is extended to $\log(\sigma_{S_j}(X_i)/\sigma_T(X_i)) = X_i^\top \omega_j$, where $\omega_1 = (0, 0.5, 0.45, -0.9, -0.7)^\top$ and $\omega_2 = (0, 0.4, 0.9, -0.5, -0.9)^\top$. We further consider

$$\frac{\sigma_S^{(q)}(X)}{\sigma_T^{(q)}(X)} = \left(\frac{\sigma_S(X)}{\sigma_T(X)} \right)^q$$

for $q = 1, 2, 3$, where q determines the degree of covariate shift with $q = 3$ signifying a large covariate shift.

In the above configurations, we specify $\eta = 0.0001, \nu = 3, \alpha = (0, 2, 1, -1.2, 0.8)^\top$, and $\eta_c = 0.0001, \nu_c = 2.7, \alpha_c = (1, 0.5, -0.5, -0.5)^\top$.

Several methods with details in Table 1 are compared. The pseudo observation mean in the target domain, serving as a benchmark for comparing all methods in terms of absolute bias

$$\text{Err}_{\mathcal{T}} = |\mathbb{E}_{\mathcal{U}_{\mathcal{T}}} \tilde{m}^{(k)}(X; t) - \tau^{(k)}(t)|$$

or relative bias $\text{Err}_{\mathcal{T}}/|\tau^{(k)}(t)|$.

5.1 Estimation bias

As expected, due to covariate-shift, NAIVE estimate of the survival probabilities or restricted mean survival time using the mean estimates from the source population shows

Table 1: Methods and their descriptions used in simulation comparisons.

NAIVE	Unweighted mean of pseudo-observations from the source domain.
IPSW	IPSW weighted mean of pseudo observations from the source domain. The propensity scores are learned using logistic regression.
IPSW-SUB	Subgroup-specific IPSW estimates, each subgroup’s propensity score learned via logistic regression.
LM	Naive linear model fitted for the source domain (without calibration), with the target domain estimate derived from the average prediction.
MCLM-RIDGE	The linear model is post-processed on the auditing set of the source using ridge regression; estimates are from the average of ridge-multi-calibrated linear predictions.
MCLM-TREE	Similar post-processing of the linear model using a decision tree; estimates are from the average of tree-multi-calibrated linear predictions.
RF	Random forest (RF) trained on the source domain, with estimates from averaged RF predictions over unlabeled target domain samples.
MCRF-RIDGE	Post-processing of the RF on the source’s auditing set using ridge regression. The average of ridge-multi-calibrated RF predictions gives the estimate.
MCRF-TREE	Similar post-processing of RF using a decision tree. The average of tree-multi-calibrated RF predictions give the estimate.

a large bias toward the target mean because the unweighted samples are not representative of the true target domain population (Figure S.8, S.9). Under mild covariate shift ($q = 1$, Figure 2), the IPSW approach alleviates the bias significantly, owing to the sample reweighting that makes nonrandom source samples look like samples drawn from the target domain. IPSW achieves an overall low bias. The proposed post-processed multicalibrated estimators exhibit comparable overall performance.

We also estimate propensity scores for each subpopulation (denoted as ‘IPSW-SUB’), which leads to reduced biases over the standard IPSW. The performance is exceptional, particularly under conditions of mild covariate shift. The rationale for this improvement is because of the method’s focused attention on subpopulations. The enhancement will be more salient if subpopulations are endowed with very different shift models. Remarkably, our calibrated estimators attain substantial improvement over conventional learning methods, including linear model and random forest, as anticipated. It mitigates the group-wise disparities, achieving competitive or lower biases for most, if not all the time points.

The absolute biases of survival probability tend to increase for later time point due to censoring, especially when there is a strong covariate shift ($q = 3$, Figure 3). Under strong covariate-shift, IPSW approaches and machine learning methods fail to provide good estimates in the target domain, whereas the multicalibrated approach performs very well and achieves fairness among groups. This Figure shows that the most accurate predictions are always from the multicalibrated post-processing estimator. We note some slight differences between calibration using ridge regression and calibration using decision trees, however, no consistent trend is observed. We observe that post-processing with

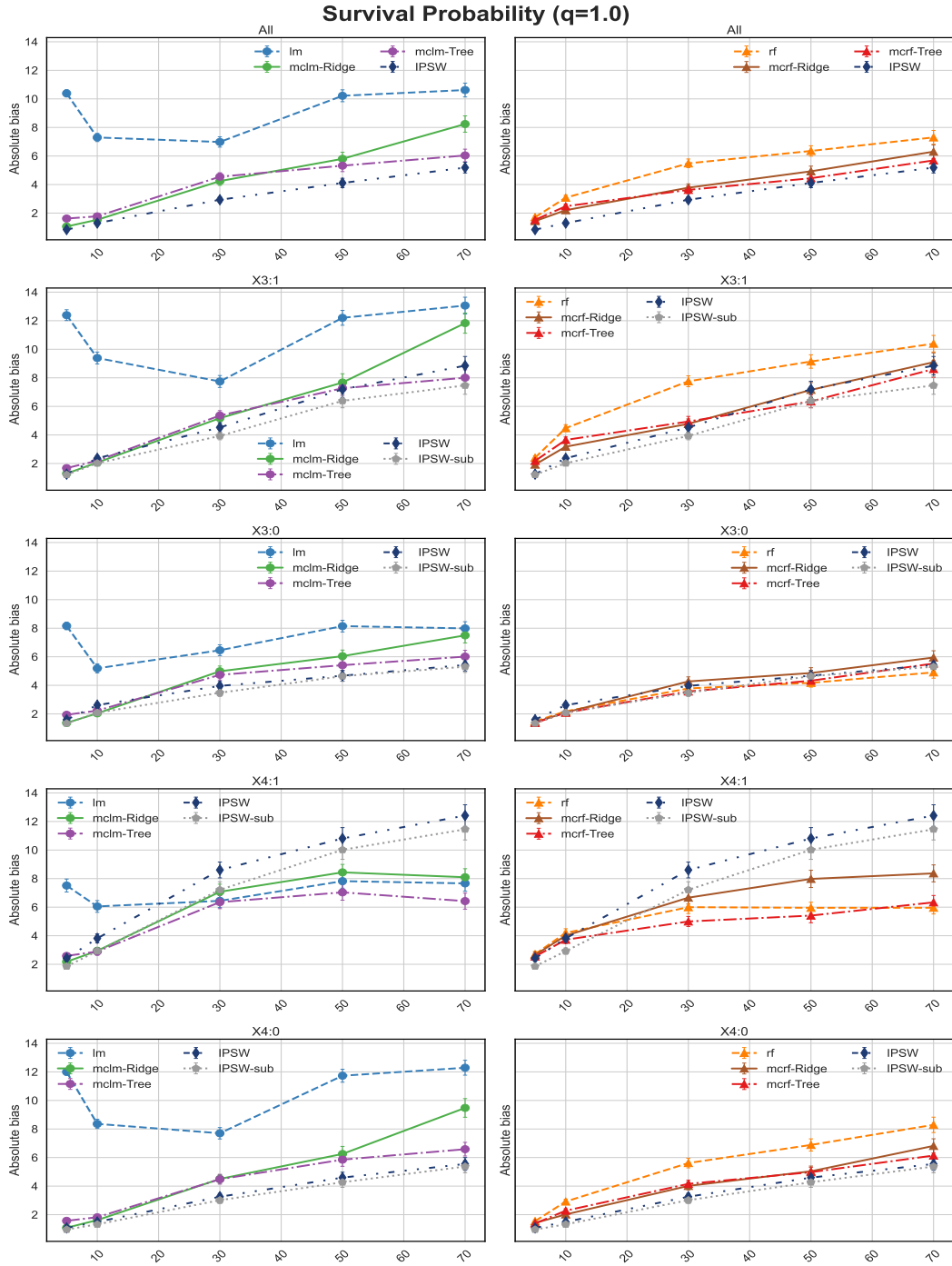


Figure 2: The absolute bias ($\times 10^2$) for all methods in estimating survival probability under mild covariate shift ($q = 1$) with a total sample size of $N = 1000$. The survival time is generated from a proportional hazard model, and the censoring is covariate-independent. Results for all subpopulations are presented based on 100 simulation replications. Left panel: linear model is used to estimate the survival probability using pseudo observations. Right panel: random forest is used to estimate the survival probability using pseudo observations.

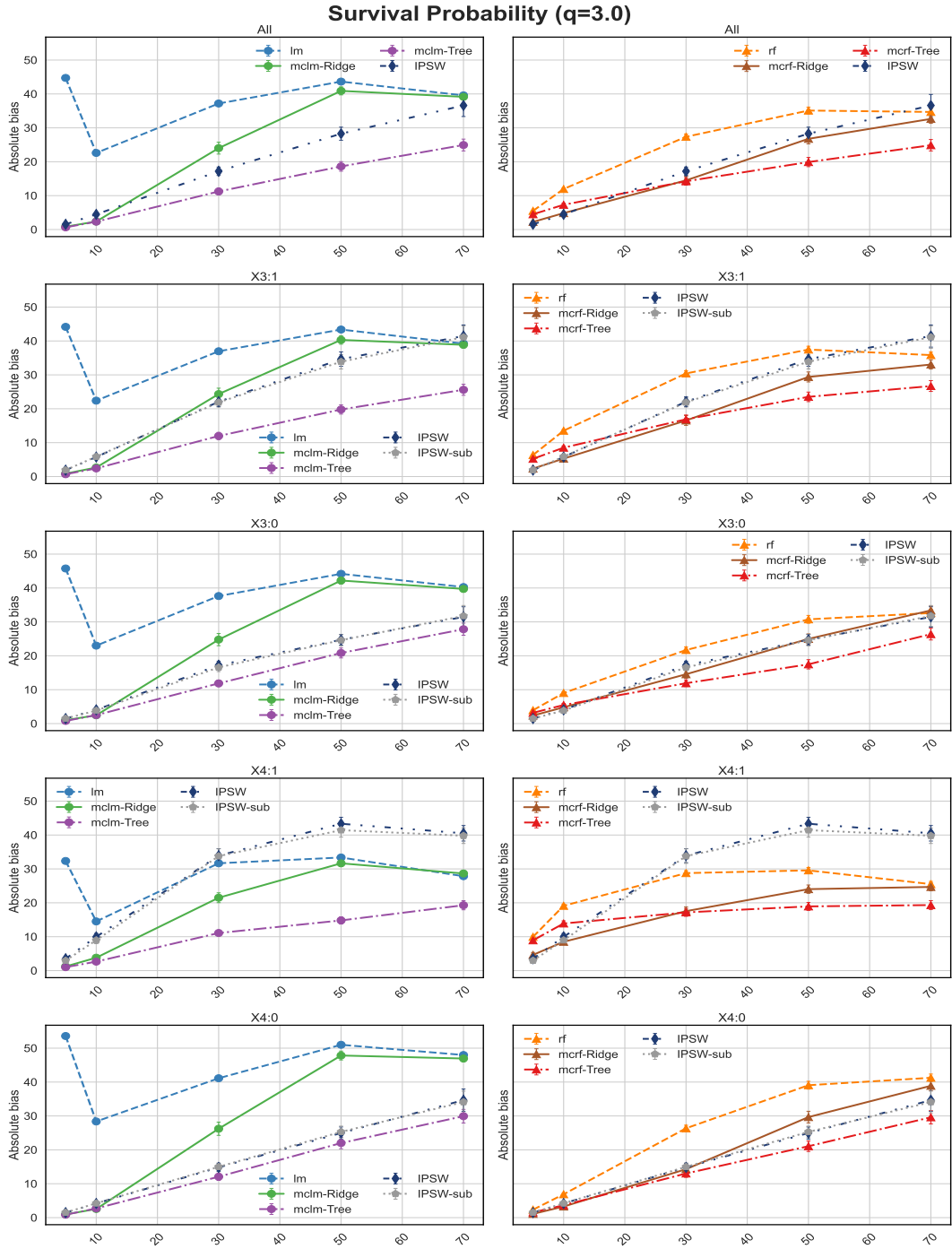


Figure 3: The absolute bias ($\times 10^2$) for all methods in estimating survival probability under mild covariate shift ($q = 3$) with a total sample size of $N = 1000$. The survival time adheres to the proportional hazard model, and the censoring is covariate-independent. Results for all subpopulations are presented based on 100 simulation replications. Left panel: linear model is used to estimate the survival probability using pseudo observations. Right panel: random forest is used to estimate the survival probability using pseudo observations.

ridge regression typically requires a small stepsize and fewer steps to convergence, and the tree requires larger stepsize and more steps. For simplicity, we employ the same stepsize $\eta = 0.3$ for all methods in Figure 3. We also observe that carefully tuning the parameters can lead to better predictions.

We observe similar results for the prediction of restricted mean (RM) $\tau^2(t) = \mathbb{E}_{\mathcal{D}_\tau}[T \wedge t]$ in the target domain, as summarized in Figures S.12 and S.14 of Section S.1. We present the relative error because the absolute error grows significantly as t increases. The multicalibrated based approaches learn and calibrate bounded functions that enjoy low prediction errors across all subpopulations, thus outperforming other competitors.

Finally, similar results are observed for estimating both the survival probability and restricted mean survival time in the target domain under moderate shift ($q = 2$), as evidenced by Figures S.9, S.11 and S.13. Due to the space limit, we refer readers to Section S.1 in the supplementary material for more details.

5.2 The concordance index

The concordance index (C-index) (Harrell et al., 1982; Harrell Jr et al., 1984) computes the agreement between the predicted survival ranking and the actual survival time, serving as an important metric for the discriminative power of the predictive model, especially involving censored observations. Specifically, it considers instance pairs and checks if the model’s prediction ranks the two instances in accordance with their true orders. The C-index takes the form

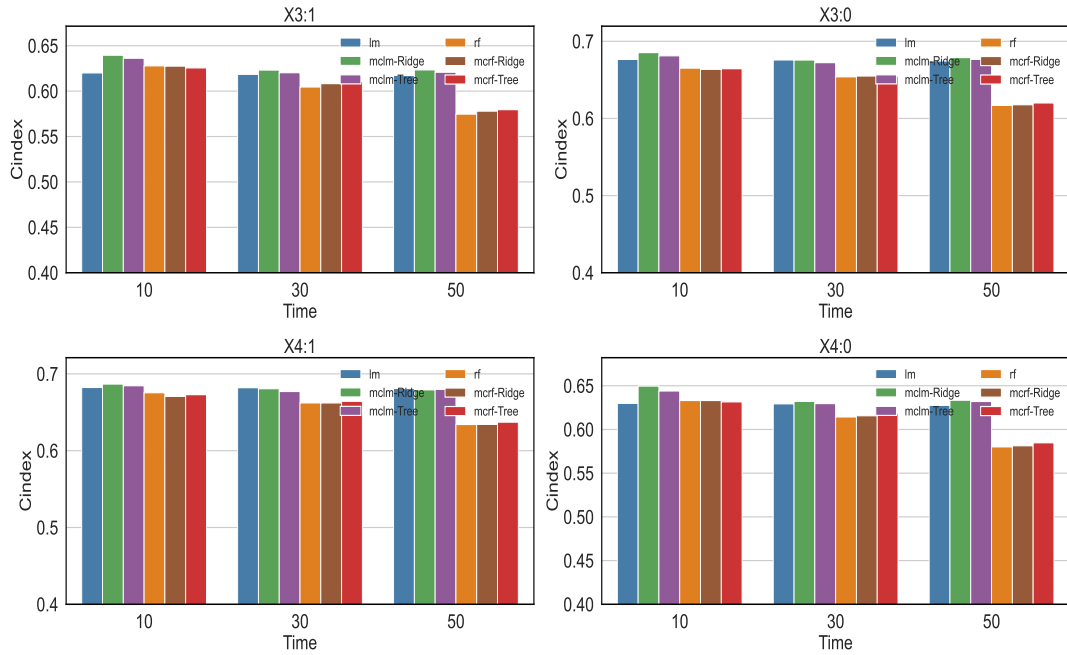
$$C(t) := \frac{\sum_{\Delta_i=1} \sum_{\tilde{T}_j > \tilde{T}_i} \mathbf{1}\{\hat{S}(t|X_j) > \hat{S}(t|X_i)\}}{\sum_{\Delta_i=1} \sum_{\tilde{T}_j > \tilde{T}_i} \mathbf{1}\{\tilde{T}_j > \tilde{T}_i\}}, \quad (10)$$

where \hat{S} is any prediction for survival probability. Each non-censored instance is compared against all instances that outlive it (having a larger event or censoring time). Each correct ranking is counted, and the final score is normalized over the total number of pairs. The C-index (10) becomes the area under the curve (AUC) for binary problem with no censoring instances (Haider et al., 2020).

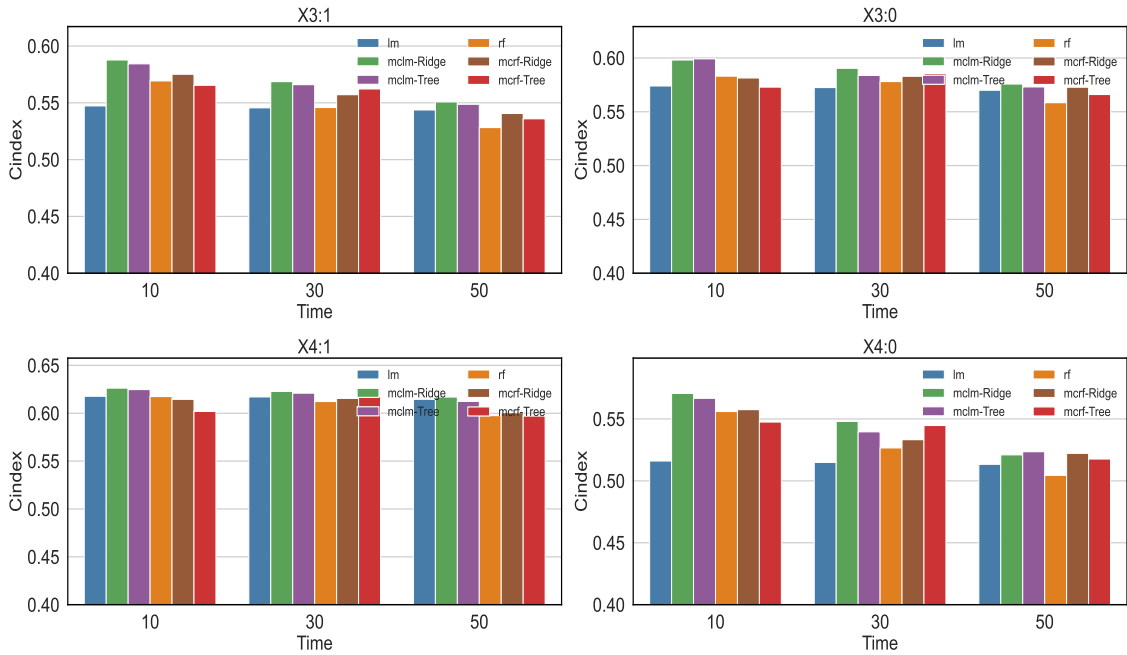
We observe that multicalibration also leads to increased C-index as illustrated in Figure 4 and Figure S.10 under strong covariate-shift, with similar performance under the weak covariate shift. Compared to random forests, the linear models result in higher C-index scores under mild covariate shift, probably attributed to the effective ranking it renders. However, it generally has higher estimation bias as supported by our simulations.

6 Application to cardiovascular disease risk prediction

We apply the methods of calibration to data from two prospective cohorts, The Multi-Ethnic Study of Atherosclerosis (MESA) (Bild et al., 2002) and The Chronic Renal Insufficiency Cohort (CRIC) (Lash et al., 2009). MESA is a population based study of the characteristics of subclinical cardiovascular disease and the risk factors that predict



(a) Mild covariate-shift ($q = 1$)



(b) strong covariate shift ($q = 3$)

Figure 4: C-index for all methods under (a) mild covariate shift ($q = 1$) and (b) strong covariate shift ($q = 3$) for various subpopulations. The proportional hazard model with independent uniform censoring is considered. Both linear model and random forest are used to estimate the survival probability using pseudo observations. Results are based on an average of 100 simulation replications.

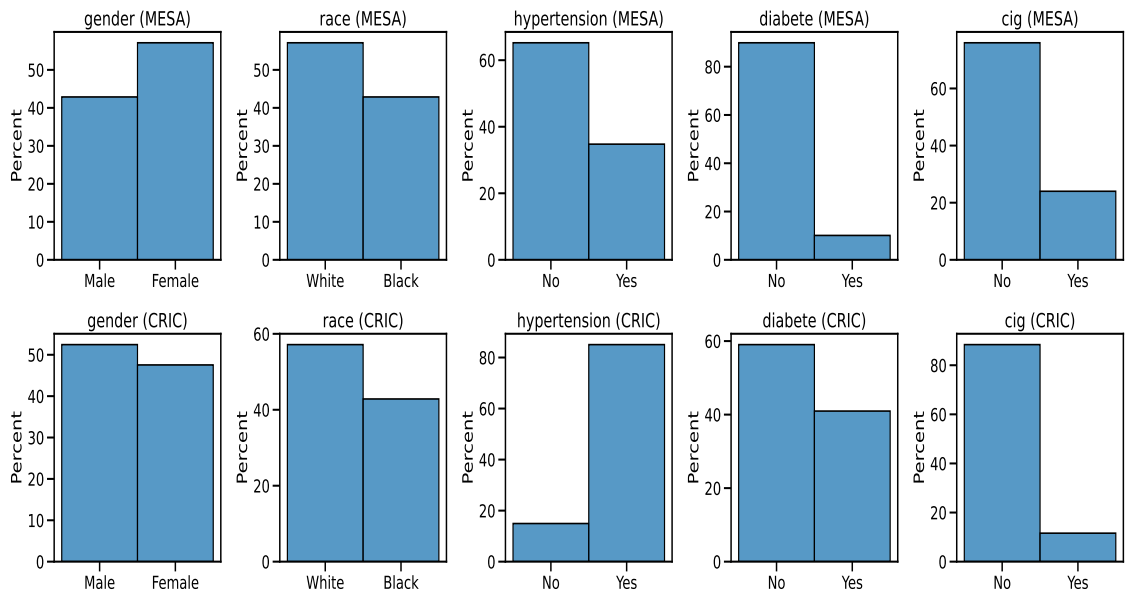


Figure 5: The boxplots of 5 categorical variables for MESA and CRIC cohorts, highlighting the presence of covariate-shift between these two cohorts.

progression to clinically overt cardiovascular disease. MESA includes a population-based sample of 6,814 asymptomatic men and women aged 45-84. In contrast, CRIC is an observational study that examines risk factors for progression of chronic renal insufficiency (CRI) and cardiovascular disease (CVD) among CRI patients. The study enrolled adults aged 21 to 74 years with a broad spectrum of renal disease severity, half of whom were diagnosed with diabetes mellitus. Both studies are interested in predicting the 10-year risk of CVD, a composite event that includes MI, cardiac arrest, confirmed angina requiring revascularization and CHD death. The time to CVD incidence is censored according to some unknown mechanism. However, substantial differences are observed in these two cohorts (Figure 5), showing evidence of a strong covariate shift among subpopulations. The CRIC cohort includes more individuals with hypertension and diabetes, suggesting a higher risk to CVD. This is further substantiated by the higher number of observed CVD events in the CRIC dataset.

In our analysis, we treat the individuals in CRIC cohort as the source data to build prediction model for 10 year CVD risk. For the testing set, since all CRIC participants had chronic kidney disease (EPIunder 60), we only use the MESA participants who had kidney disease to estimate the 10-year CVD risk. After excluding the samples with missing values and focusing on the Caucasian and black race, we obtain datasets with 1514 source samples from CRIC study and 383 target samples from MESA study. Altogether, we have 13 variables, including 5 categorical (e.g., gender, race, hypertension status, diabetic status) and 8 continuous (e.g., age, BMI, blood pressure) factors. We aim to predict the survival probability for the MESA cohort with CKI using the CRIC cohort as the source data. Our preliminary findings show that, while survival times vary between the two datasets, their restricted mean survival times are remarkably similar, a phenomenon potentially attributable to the low incidence of CVD events.

For each subgroup (gender, race, etc.), we first establish a baseline using the pseudo

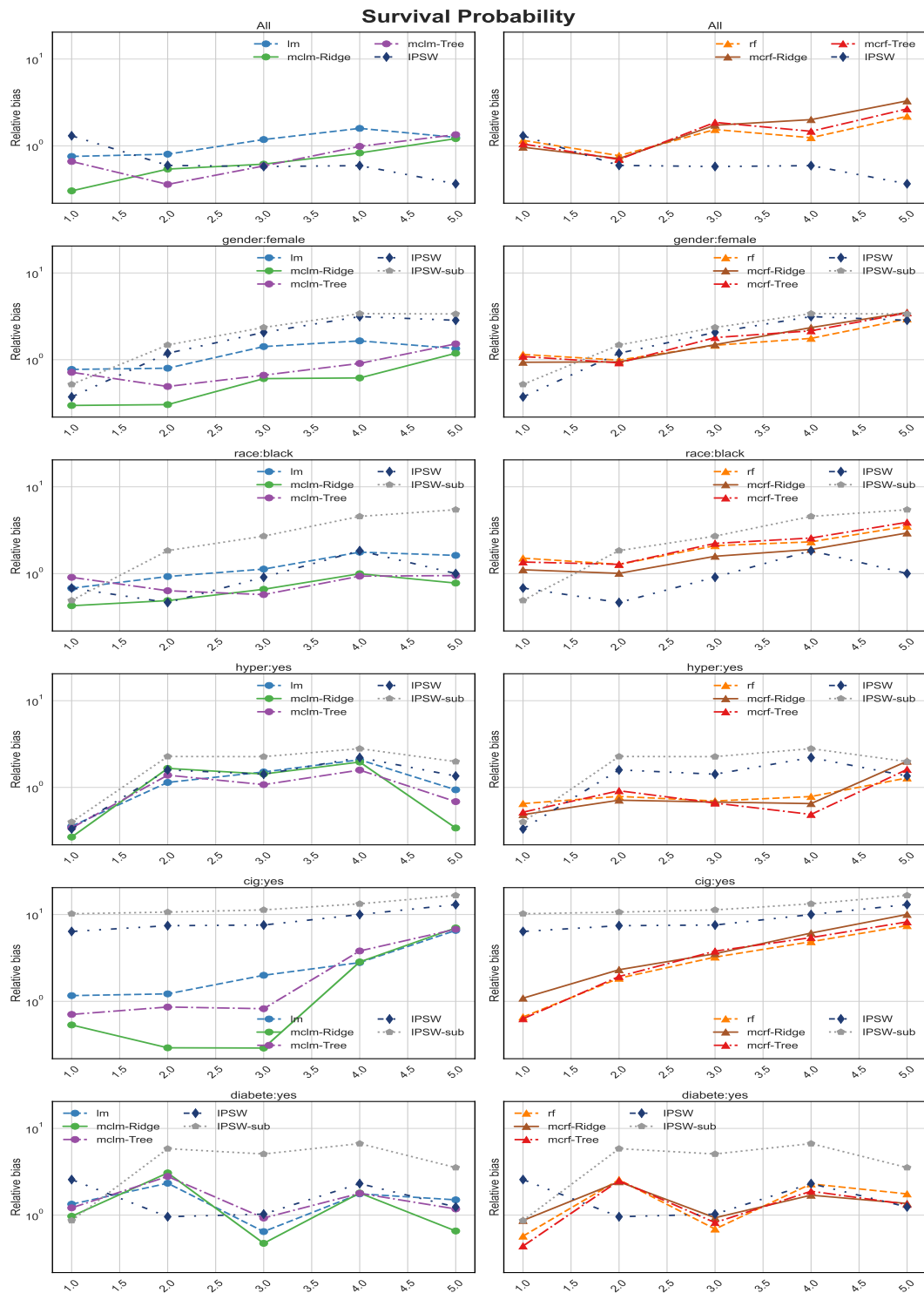


Figure 6: The relative error of all methods to predict the survival probability for all MESA cohort and various subpopulations at different follow-up time points.

observation mean over samples belonging to the group. We then evaluate the performance of IPSW and various prediction functions, both naive (linear model, random forests) and multicalibrated predictions, in estimating the survival probabilities in MESA using CRIC

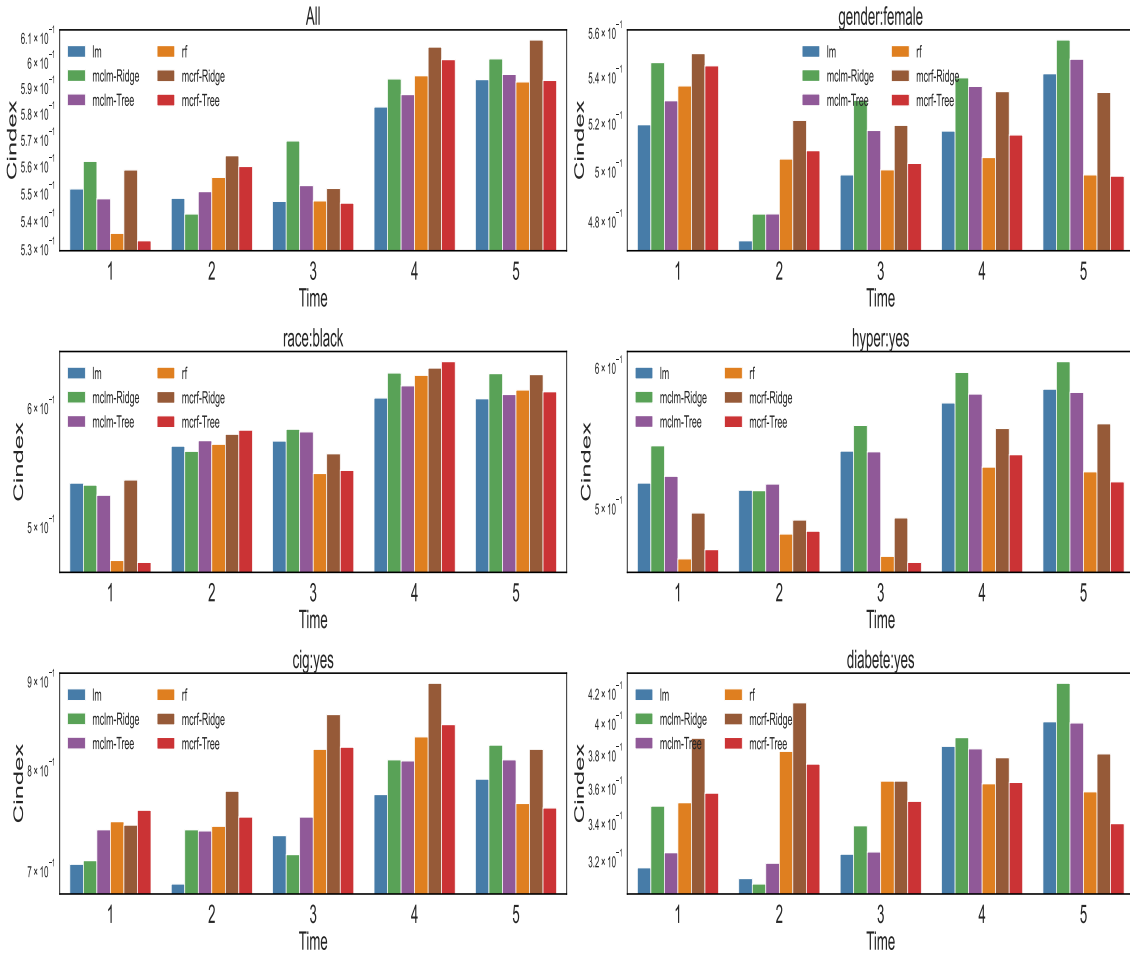


Figure 7: C-index (in log scale) of predicting survival probability from different methods for all MESA cohort and various subpopulations at different follow-up time points.

data. We also evaluate the prediction performance using the concordance index (C-index) that serves as an additional metric for assessing models’ discriminative ability.

We report the prediction error for each method in Figure 6. It shows that naive estimation using source data alone leads to substantial prediction errors due to the large difference in covariate distributions between the source CRIC and target MESA cohorts. In contrast, methods that are post-processed to be multicalibrated consistently demonstrate lower prediction errors compared to their uncalibrated counterparts and outperform the IPSW approach.

Given the low incidence of CVD in both cohorts, the C-index in general is not very high. However, the C-index across various subpopulations as shown in Figure 7 clearly indicates that the multicalibrated methods result in higher or similar C-index that the methods with no calibration.

These results agree with our simulation findings, highlighting the improvement from a single multicalibrated prediction function trained on source data in generalizing the results to unknown target population. Such performances are competitive with shift-specific methods as well as traditional machine learning algorithms. The strong performance

across diverse subpopulations illuminates the connection between universal adaptability and the concept of multicalibration: a multicalibrated predictor must robustly model outcome variations, not merely on an aggregate level but across multiple subpopulations. This highlights the potential of multicalibration as a tool to achieve similar predictive performance in diverse and shifting populations.

References

- Andersen, P. K. and Pohar Perme, M. (2010). Pseudo-observations in survival analysis. *Statistical methods in medical research*, 19(1):71–99.
- Bellot, A. and van der Schaar, M. (2019). Boosting transfer learning with survival data from heterogeneous domains. In *The 22nd International Conference on Artificial Intelligence and Statistics*, pages 57–65. PMLR.
- Bickel, S., Brückner, M., and Scheffer, T. (2009). Discriminative learning under covariate shift. *Journal of Machine Learning Research*, 10(9).
- Bild, D. E., Bluemke, D. A., Burke, G. L., Detrano, R., Diez Roux, A. V., Folsom, A. R., Greenland, P., Jacobs Jr., D. R., Kronmal, R., Liu, K., Nelson, J. C., O’Leary, D., Saad, M. F., Shea, S., Szklo, M., and Tracy, R. P. (2002). Multi-Ethnic Study of Atherosclerosis: Objectives and Design. *American Journal of Epidemiology*, 156(9):871–881.
- Binder, N., Gerds, T. A., and Andersen, P. K. (2014). Pseudo-observations for competing risks with covariate dependent censoring. *Lifetime data analysis*, 20:303–315.
- Buolamwini, J. and Gebru, T. (2018). Gender shades: Intersectional accuracy disparities in commercial gender classification. In *Conference on fairness, accountability and transparency*, pages 77–91. PMLR.
- Cole, S. R. and Stuart, E. A. (2010). Generalizing evidence from randomized clinical trials to target populations: the actg 320 trial. *American journal of epidemiology*, 172(1):107–115.
- Cox, D. R. (1972). Regression models and life-tables. *Journal of the Royal Statistical Society: Series B (Methodological)*, 34(2):187–202.
- Davison, A. C. (2003). *Statistical models*, volume 11. Cambridge university press.
- Deng, Z., Dwork, C., and Zhang, L. (2023). Happymap: A generalized multi-calibration method. *arXiv preprint arXiv:2303.04379*.
- Dudley, R. M. and Norvaiša, R. (1999). *Differentiability of six operators on nonsmooth functions and p-variation*. Number 1703.
- Dudley, R. M., Norvaiša, R., and Norvaiša, R. (2011). *Concrete functional calculus*. Springer.

- Dudley, R. M. and Philipp, W. (1983). Invariance principles for sums of banach space valued random elements and empirical processes. *Zeitschrift für Wahrscheinlichkeitstheorie und verwandte Gebiete*, 62(4):509–552.
- Dwork, C., Hardt, M., Pitassi, T., Reingold, O., and Zemel, R. (2012). Fairness through awareness. In *Proceedings of the 3rd innovations in theoretical computer science conference*, pages 214–226.
- Efron, B. and Hastie, T. (2021). *Computer age statistical inference, student edition: algorithms, evidence, and data science*, volume 6. Cambridge University Press.
- Frangakis, C. (2009). The calibration of treatment effects from clinical trials to target populations.
- Goldstein, M., Han, X., Puli, A., Perotte, A., and Ranganath, R. (2020). X-cal: Explicit calibration for survival analysis. *Advances in neural information processing systems*, 33:18296–18307.
- Graw, F., Gerds, T. A., and Schumacher, M. (2009). On pseudo-values for regression analysis in competing risks models. *Lifetime data analysis*, 15:241–255.
- Guntuboyina, A. and Sen, B. (2012). L1 covering numbers for uniformly bounded convex functions. In *Conference on Learning Theory*, pages 12–1. JMLR Workshop and Conference Proceedings.
- Haider, H., Hoehn, B., Davis, S., and Greiner, R. (2020). Effective ways to build and evaluate individual survival distributions. *Journal of Machine Learning Research*, 21(85):1–63.
- Harrell, F. E., Califf, R. M., Pryor, D. B., Lee, K. L., and Rosati, R. A. (1982). Evaluating the yield of medical tests. *Jama*, 247(18):2543–2546.
- Harrell Jr, F. E., Lee, K. L., Califf, R. M., Pryor, D. B., and Rosati, R. A. (1984). Regression modelling strategies for improved prognostic prediction. *Statistics in medicine*, 3(2):143–152.
- Hebert-Johnson, U., Kim, M., Reingold, O., and Rothblum, G. (2018). Multicalibration: Calibration for the (Computationally-identifiable) masses. In Dy, J. and Krause, A., editors, *Proceedings of the 35th International Conference on Machine Learning*, volume 80 of *Proceedings of Machine Learning Research*, pages 1939–1948. PMLR.
- Jacobsen, M. and Martinussen, T. (2016). A note on the large sample properties of estimators based on generalized linear models for correlated pseudo-observations. *Scandinavian Journal of Statistics*, 43(3):845–862.
- James, L. F. (1997). A study of a class of weighted bootstraps for censored data. *The Annals of Statistics*, 25(4):1595–1621.
- Kamran, F. and Wiens, J. (2021). Estimating calibrated individualized survival curves with deep learning. In *Proceedings of the AAAI Conference on Artificial Intelligence*, volume 35, pages 240–248.

- Kim, M. P., Ghorbani, A., and Zou, J. (2019). Multiaccuracy: Black-box post-processing for fairness in classification. In *Proceedings of the 2019 AAAI/ACM Conference on AI, Ethics, and Society*, pages 247–254.
- Kim, M. P., Kern, C., Goldwasser, S., Kreuter, F., and Reingold, O. (2022). Universal adaptability: Target-independent inference that competes with propensity scoring. *Proceedings of the National Academy of Sciences*, 119(4).
- Kuelbs, J. (1977). Kolmogorov’s law of the iterated logarithm for banach space valued random variables. *Illinois Journal of Mathematics*, 21(4):784–800.
- Lash, J. P., Go, A. S., Appel, L. J., He, J., Ojo, A., Rahman, M., Townsend, R. R., Xie, D., Cifelli, D., Cohan, J., Fink, J. C., Fischer, M. J., Gadegbeku, C., Hamm, L. L., Kusek, J. W., Landis, J. R., Narva, A., Robinson, N., Teal, V., and Feldman, H. I. a. R. I. C. C. S. G. (2009). Chronic renal insufficiency cohort (cric) study: baseline characteristics and associations with kidney function. *Clinical journal of the American Society of Nephrology : CJASN*, 4(8):1302–1311.
- Li, Z., Shen, Y., and Ning, J. (2023). Accommodating time-varying heterogeneity in risk estimation under the cox model: A transfer learning approach. *Journal of the American Statistical Association*, 118(544):2276–2287.
- Miller, R. G. (1974). The jackknife—a review. *Biometrika*, 61(1):1–15.
- Moreno-Torres, J. G., Raeder, T., Alaiz-Rodríguez, R., Chawla, N. V., and Herrera, F. (2012). A unifying view on dataset shift in classification. *Pattern recognition*, 45(1):521–530.
- Overgaard, M., Parner, E. T., and Pedersen, J. (2017). Asymptotic theory of generalized estimating equations based on jack-knife pseudo-observations. *The Annals of Statistics*, pages 1988–2015.
- Overgaard, M., Parner, E. T., and Pedersen, J. (2019). Pseudo-observations under covariate-dependent censoring. *Journal of Statistical Planning and Inference*, 202:112–122.
- Pfisterer, F., Kern, C., Dandl, S., Sun, M., Kim, M. P., and Bischl, B. (2021). mcboost: Multi-calibration boosting for r. *Journal of Open Source Software*, 6(64):3453.
- Qian, J. (1998). The p -variation of partial sum processes and the empirical process. *The Annals of Probability*, 26(3):1370–1383.
- Roth, A. (2022). Uncertain: Modern topics in uncertainty estimation.
- Rubin, D. B. (1974). Estimating causal effects of treatments in randomized and nonrandomized studies. *Journal of educational Psychology*, 66(5):688.
- Shaker, A. and Lawrence, C. (2023). Multi-source survival domain adaptation. In *Proceedings of the AAAI Conference on Artificial Intelligence*, volume 37, pages 9752–9762.

- Vaart, A. W. v. d. (1998). *Asymptotic Statistics*. Cambridge Series in Statistical and Probabilistic Mathematics. Cambridge University Press.
- Vershynin, R. (2018). *High-Dimensional Probability: An Introduction with Applications in Data Science*. Cambridge Series in Statistical and Probabilistic Mathematics. Cambridge University Press.
- Wainwright, M. J. (2019). *High-Dimensional Statistics: A Non-Asymptotic Viewpoint*. Cambridge Series in Statistical and Probabilistic Mathematics. Cambridge University Press.
- Wei, L.-J. (1992). The accelerated failure time model: a useful alternative to the cox regression model in survival analysis. *Statistics in medicine*, 11(14-15):1871–1879.
- Weisberg, H. I., Hayden, V. C., and Pontes, V. P. (2009). Selection criteria and generalizability within the counterfactual framework: explaining the paradox of antidepressant-induced suicidality? *Clinical trials*, 6(2):109–118.
- Zeng, S., Li, F., and Hu, L. (2021). Propensity score weighting analysis of survival outcomes using pseudo-observations. *arXiv preprint arXiv:2103.00605*.
- Zhang, X., Zhou, H., and Ye, H. (2022). A modern theory for high-dimensional cox regression models. *arXiv preprint arXiv:2204.01161*.

Supplementary Materials for “Multicalibration for Modeling Censored Survival Data with Universal Adaptability”

S.1 Additional Simulations

We have carried out additional simulations that are complementary to the main body of the paper. These simulations were designed to explore different scenarios with varying parameter configurations ($t \in \{5, 10, 30, 50, 70\}$, $q = 1, 2, 3$), thus providing a comprehensive understanding of our model under different conditions. As supplementary to the main content, Figures S.8, S.9 depict the improvement of IPSW over naive approach, and Figures S.10-S.11 present results for moderate shift, and Figures S.12 through S.14 display outcome for RM.

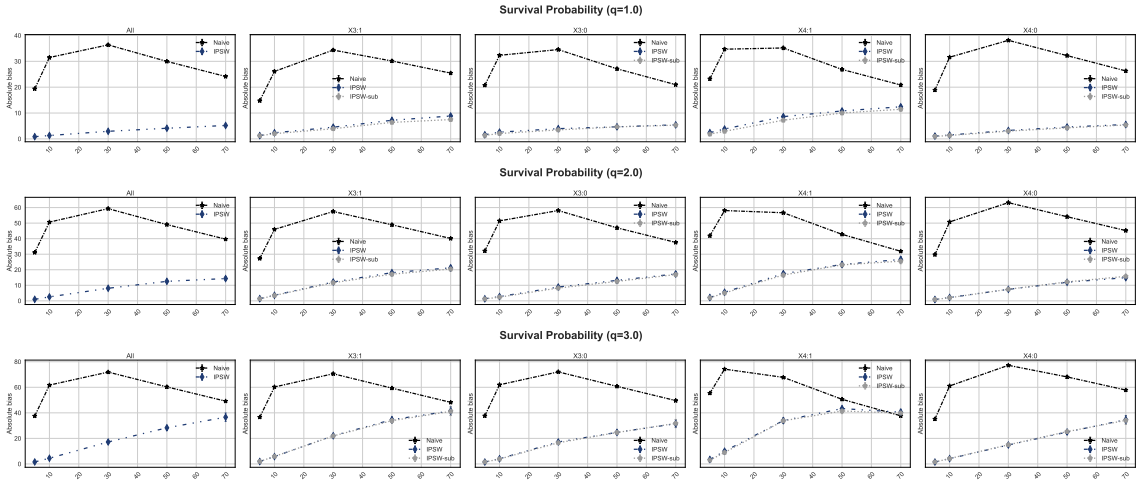


Figure S.8: The absolute bias ($\times 10^2$) for ‘Naive,’ ‘IPSW,’ and ‘IPSW-sub’ in estimating survival probability under varying degrees of covariate shift ($q = 1, 2, 3$), with a total sample size of $N = 1000$. The survival time adheres to the proportional hazard model, and the censoring is covariate-independent. Results are aggregated from 100 simulation replications for all subpopulations.

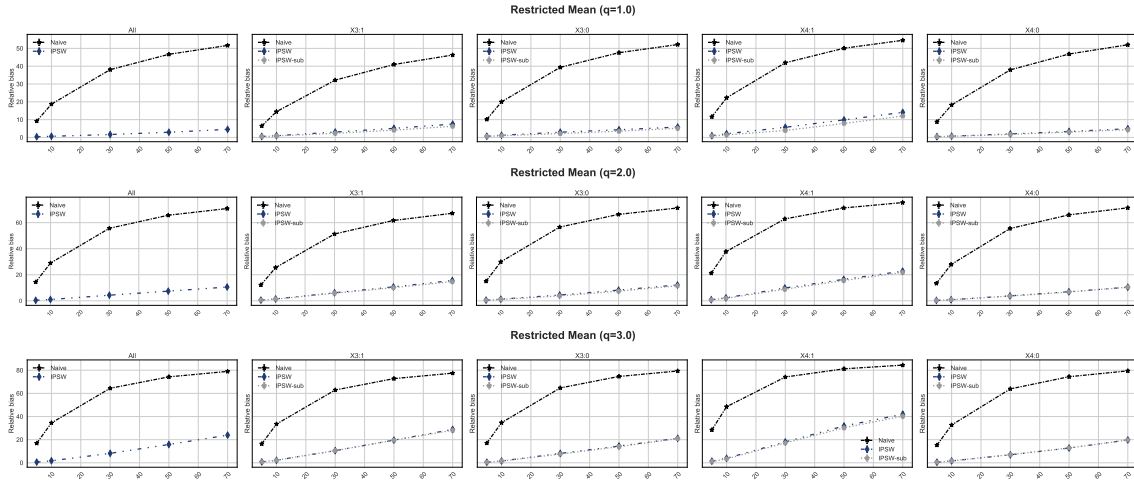


Figure S.9: The relative bias ($\times 10^2$) for ‘Naive,’ ‘IPSW,’ and ‘IPSW-sub’ in estimating restricted mean under varying degrees of covariate shift ($q = 1, 2, 3$), with a total sample size of $N = 1000$. The survival time adheres to the proportional hazard model, and the censoring is covariate-independent. Results are aggregated from 100 simulation replications for all subpopulations.

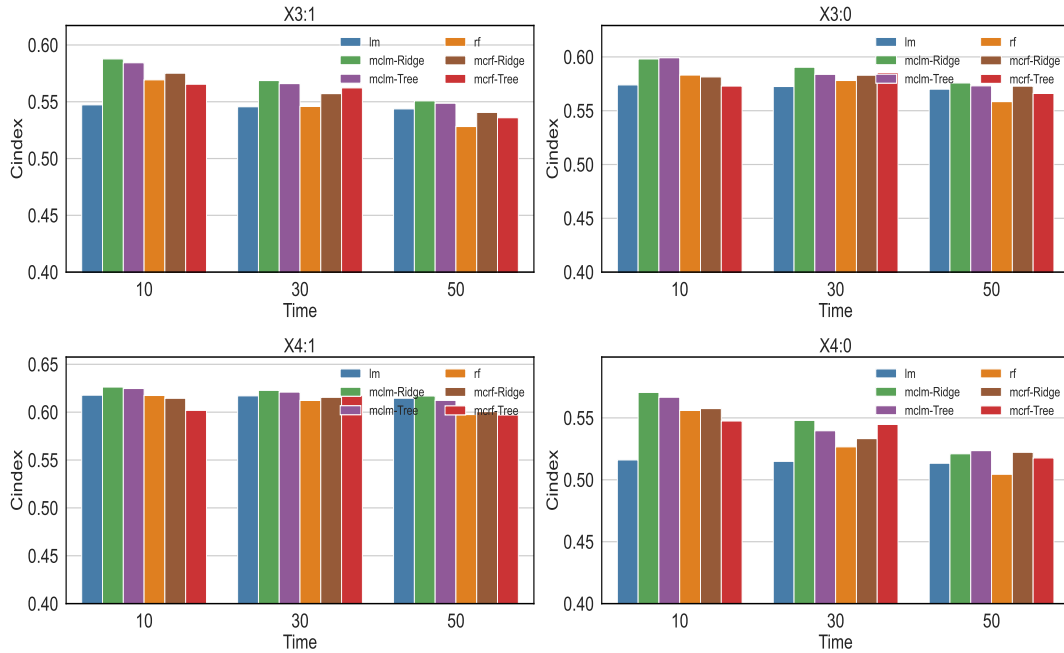


Figure S.10: C-index for all methods under moderate covariate shift ($q = 2$) for various subpopulations. The proportional hazard model with independent censoring following a uniform distribution is considered. Results are based on an average of 100 simulation replications.

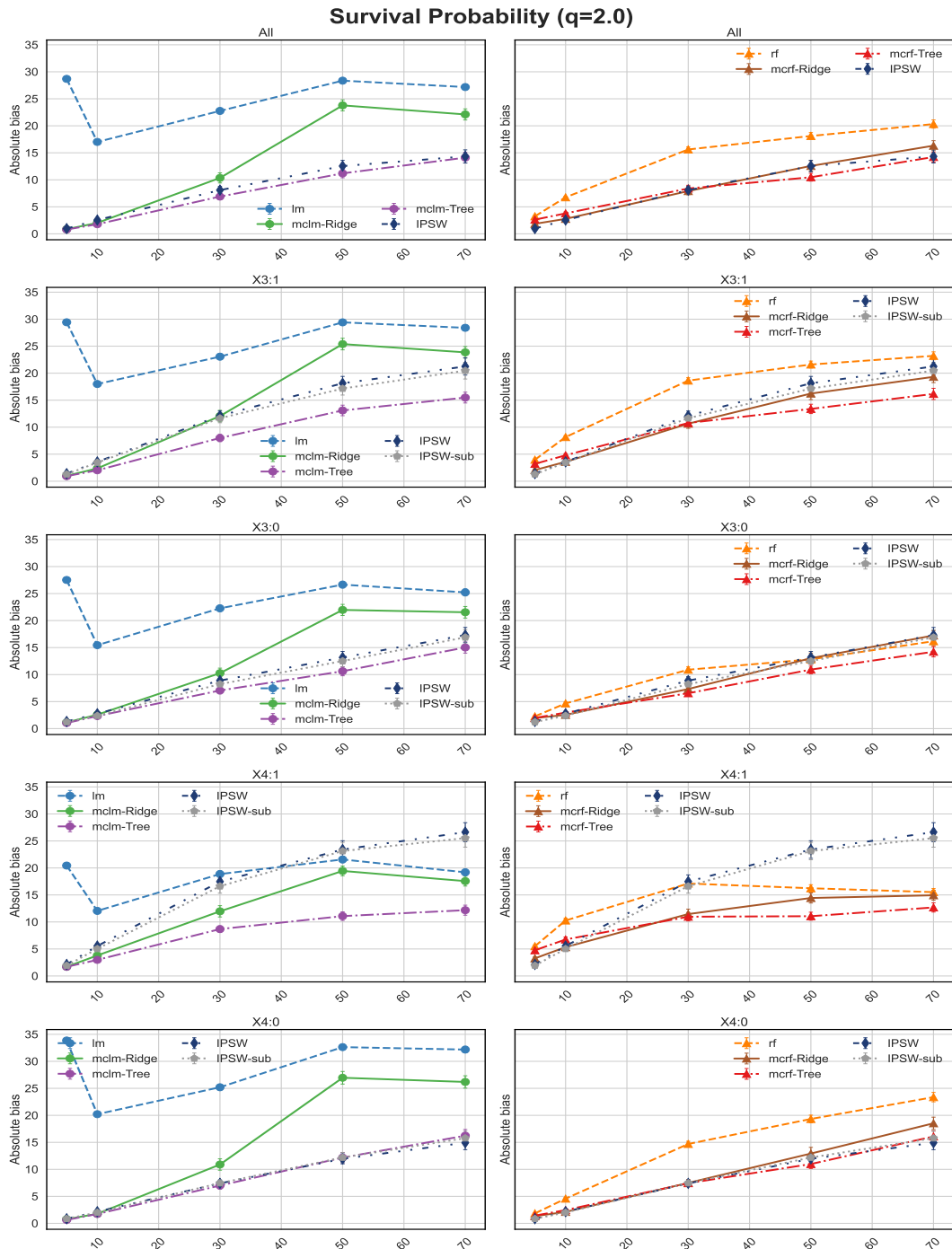


Figure S.11: The absolute bias ($\times 10^2$) for all methods in estimating survival probability under mild covariate shift ($q = 2$) with a total sample size of $N = 1000$. The survival time adheres to the proportional hazard model, and the censoring is covariate-independent. Results for all subpopulations are presented based on 100 simulation replications.

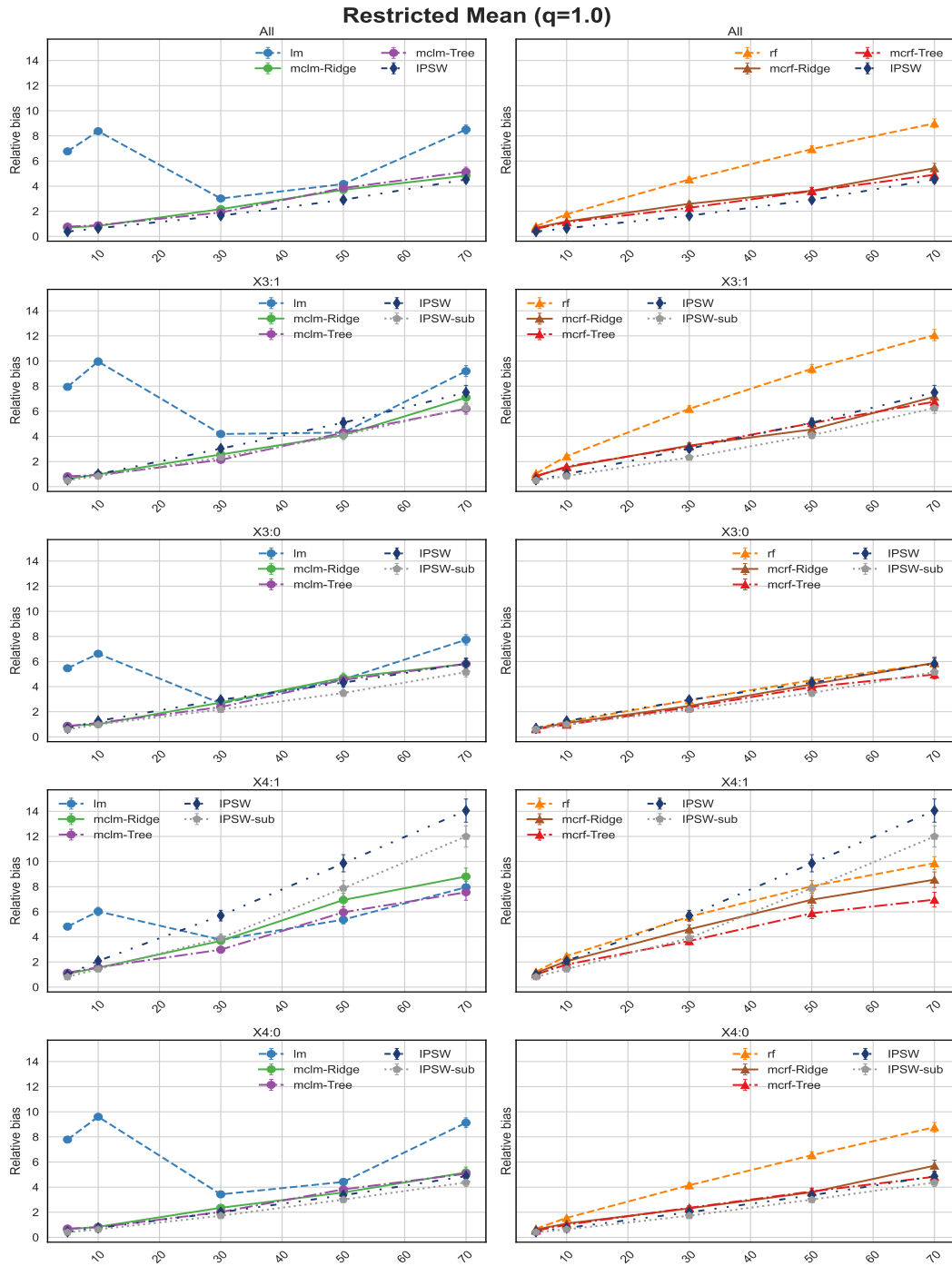


Figure S.12: The relative bias ($\times 10^2$) for all methods in estimating restricted survival mean time under mild covariate shift ($q = 1$) with a total sample size of $N = 1000$. The survival time adheres to the proportional hazard model, and the censoring is covariate-independent. Results for all subpopulations are presented based on 100 simulation replications.

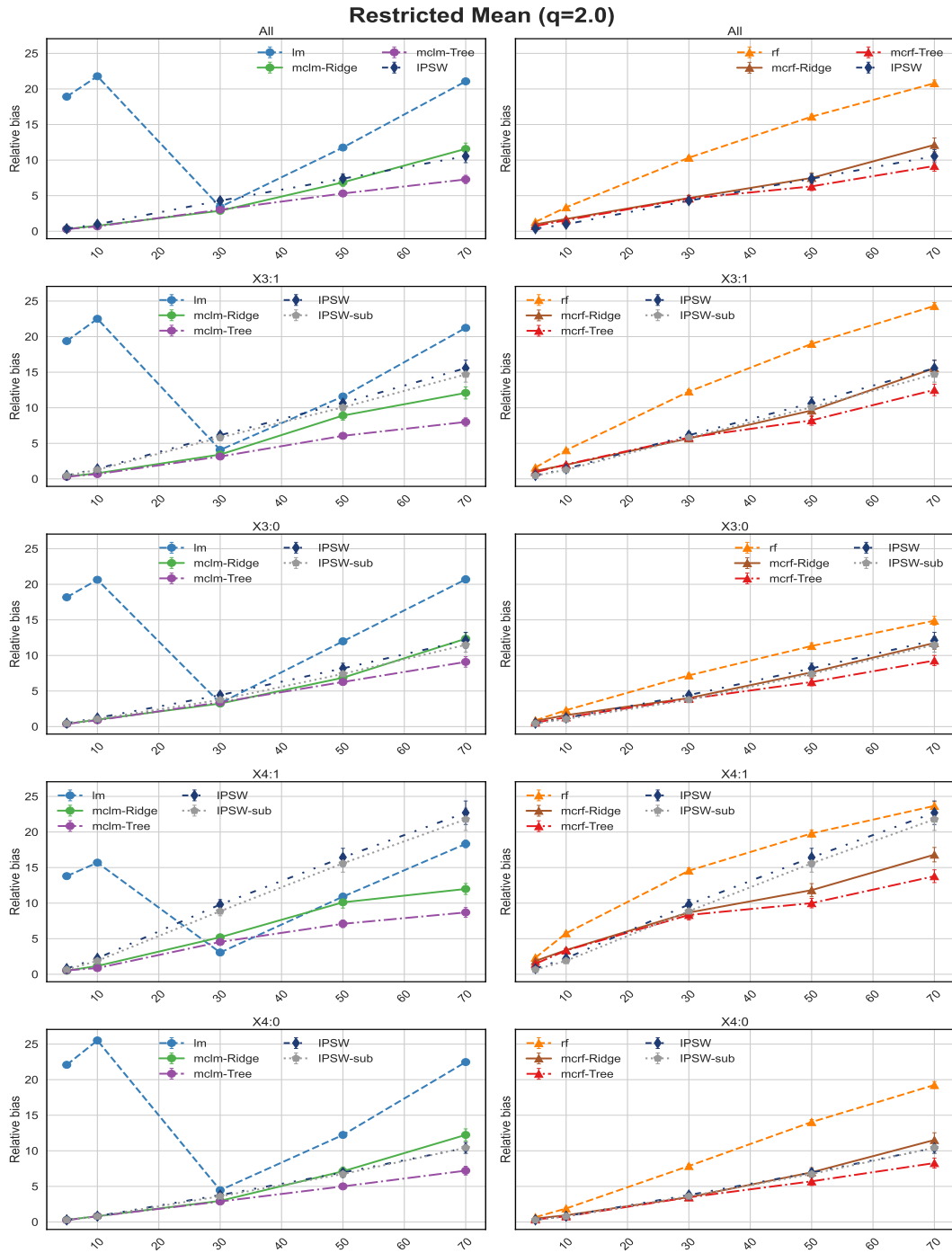


Figure S.13: The relative bias ($\times 10^2$) for all methods in estimating the restricted survival mean time under strong covariate shift ($q = 2$) with a total sample size of $N = 1000$. The survival time adheres to the proportional hazard model, and the censoring is covariate-independent. Results for all subpopulations are presented based on 100 simulation replications.

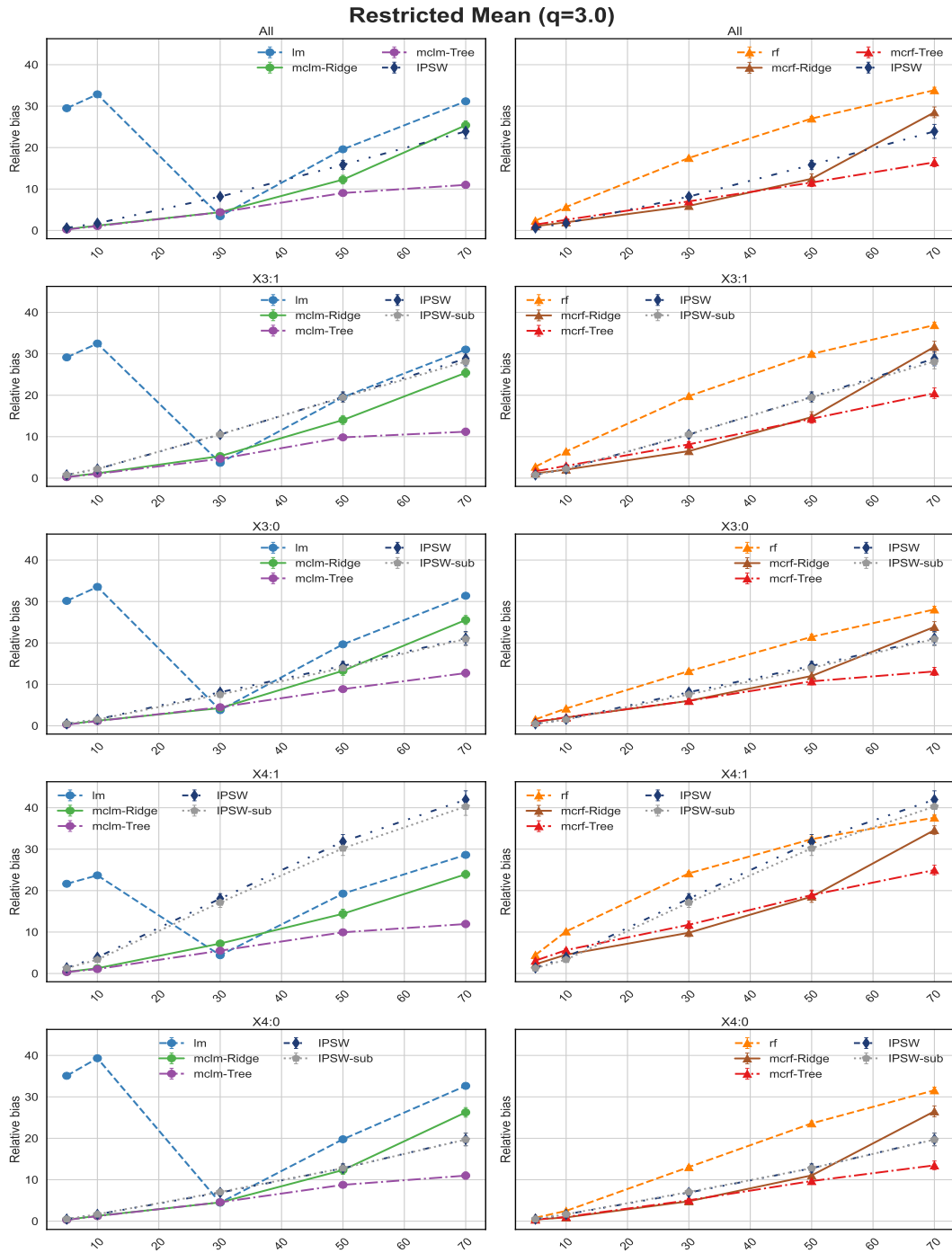


Figure S.14: The relative bias ($\times 10^2$) for all methods in estimating the restricted survival mean time under strong covariate shift ($q = 3$) with a total sample size of $N = 1000$. The survival time adheres to the proportional hazard model, and the censoring is covariate-independent. Results for all subpopulations are presented based on 100 simulation replications.